AD-A133 658 OPTICAL ANALOG REPEATER DEVELOPMENT FOR A ONE GHZ BANDWIDTH RECIRCULATING DELAY LINE(U) TRW TECHNOLOGY RESEARCH CENTER EL SEGUNDO CA T V MUOI SEP 83 1/1

UNCLASSIFIED N00014-82-C-2285 F/G 9/1 NL

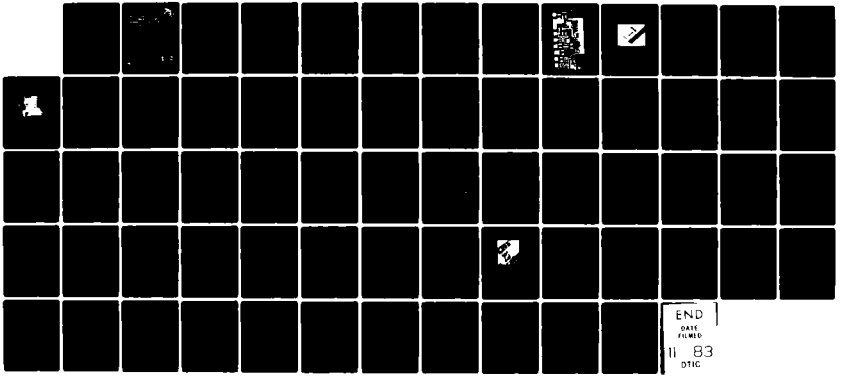

END
DATE FILMED
11 83
DTIC

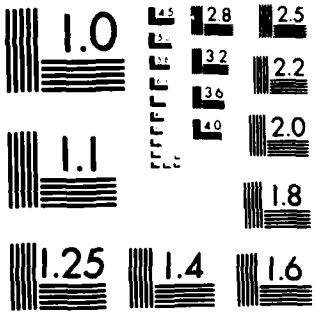

AD-133 658

FINAL REPORT

OPTICAL ANALOG REPEATER DEVELOPMENT FOR A ONE GHz BANDWIDTH RECIRCULATING DELAY LINE

REPORT NO. N00014-82-C-2285

26 SEPTEMBER 1983

Prepared for

NAVAL RESEARCH LABORATORY
WASHINGTON, DC 20375

Approved for Public Release, Distribution Unlimited

T.V. MUOI

Unclassified

SECURITY CLASSIFICATION OF THIS PAGE (When Data Entered)

REPORT DOCUMENTATION PAGE		READ INSTRUCTIONS BEFORE COMPLETING FORM
1. REPORT NUMBER N00014-82-C-2285	2. GOVT ACCESSION NO. A133658	3. RECIPIENT'S CATALOG NUMBER
4. TITLE (and Subtitle) Optical Analog Repeater Development for a 1 GHz Bandwidth Recirculating Delay Line		5. TYPE OF REPORT & PERIOD COVERED Final Report Aug '82-Aug '83 6. PERFORMING ORG. REPORT NUMBER
7. AUTHOR(s) T.V. Muoi		8. CONTRACT OR GRANT NUMBER(s) N00014-82-C-2285
9. PERFORMING ORGANIZATION NAME AND ADDRESS TRW Technology Research Center 2525 E. El Segundo Boulevard El Segundo, California 90245		10. PROGRAM ELEMENT, PROJECT, TASK AREA & WORK UNIT NUMBERS
11. CONTROLLING OFFICE NAME AND ADDRESS Naval Research Laboratory Washington, D.C. 20375		12. REPORT DATE September 1983 13. NUMBER OF PAGES 62
14. MONITORING AGENCY NAME & ADDRESS(if different from Controlling Office)		15. SECURITY CLASS. (of this report) Unclassified 15a. DECLASSIFICATION/DOWNGRADING SCHEDULE

16. DISTRIBUTION STATEMENT (of this Report)

Approved for Public Release - Distribution Unlimited

17. DISTRIBUTION STATEMENT (of the abstract entered in Block 20, if different from Report)

18. SUPPLEMENTARY NOTES

19. KEY WORDS (Continue on reverse side if necessary and identify by block number)

- Optical Analog Repeater
- High Sensitivity Wideband Optical Receiver
- Fiber Optic Recirculating Delay Line

20. ABSTRACT (Continue on reverse side if necessary and identify by block number)

The feasibility of using single mode fibers as the delay medium for a recirculating delay line of 1 GHz bandwidth and 1 ms delay time is investigated both theoretically and practically. Expected performances at both 1.3 μm and 1.5 μm wavelength with state-of-the-art optical components are indicated. Several key components that are essential for the delay line realization have been demonstrated. Optical receivers and transmitters with bandwidth exceeding 2 GHz have been achieved.

DD FORM 1 JAN 73 1473 EDITION OF 1 NOV 65 IS OBSOLETE

Unclassified

SECURITY CLASSIFICATION OF THIS PAGE (When Data Entered)

Table of Contents

1. INTRODUCTION

This report is the Final Report of a twelve-month program to develop an analog optical repeater for a 1 GHz-bandwidth recirculating delay line. The work was conducted at the TRW Technology Research Center with Dr. T.V. Muoi being the principal investigator. The program was completed in August 1983. The work was sponsored by the Naval Research Laboratory under contract number N00014-82-C-2285.

The work carried out in this report follows the previous phase of the program (under contract N00014-82-C-2412 with the Naval Research Laboratory). This previous contract involves the analytical study of the feasibility of realizing a 1 GHz bandwidth, 1 ms delay time using single mode fibers as the delay medium in a recirculating configuration. In this report, we extend the previous study in order to arrive at necessary performance and specifications, for the laser transmitter, single mode fiber and optical receiver. The trade-off between operating at 1.3 μm and 1.55 μm wavelength will be discussed. In addition, several key components necessary for the delay line realization, namely the optical receiver and laser transmitter, will be demonstrated with performance exceeding the required specifications. All this effort points toward the practical feasibility of realizing the 1 GHz-1ms delay line.

In Section 2, we present the design and experimental performances of two prototypes of the low noise optical receiver. Then in Section 3, the extended system design is reported together with the key component specifications. Both cases of 1.3 μm and 1.55 μm wavelength operation are discussed. In Section 4, we report on the design and performance of a laser transmitter breadboard. Finally, in Section 5, we present our conclusions and implications of the work carried out in this report.

2. 1.3 μm OPTICAL RECEIVER AMPLIFIER

2.1 Design

The 1.3 μm optical receiver amplifier consists of a 1.3 μm p-i-n photodiode followed by a low noise receiver amplifier. The two most important requirements on the receiver amplifier are its frequency response and noise performance. The frequency response is required to be flat to ± 0.25 dB up to 1 GHz. The input equivalent noise resistance averaged over the 0-1GHz band is required to be greater than 100 ohms.

The receiver amplifier design follows the design carried out under the previous phase of the program (NRL contract number N00014-82-C-2412 "1 GHz Bandwidth Recirculating Optical Analog Repeater"). A schematic of the receiver amplifier is shown in Figure 1. The amplifier configuration is based on the design technique of mismatching interstage coupling so that effects of stray capacitances are minimized. The first stage is a shunt-feedback transimpedance stage with a feedback resistance of 400 Ω nominal. Capacitance C_F which includes stray capacitance of the feedback resistance is used to trim the amplifier high frequency response. The second stage has a series-feedback configuration, with a collector load resistance of 50 ohms so that a good impedance match to the amplifier 50 ohm load is obtained. Both transistors are silicon microwave transistors (NE64400 from NEC) with cut-off frequency f_T of over 10 GHz.

The optimum bias current of the first transistor Q_1 for lowest amplifier noise is calculated to be about 3 mA. However, in order to avoid any possible reduction in the transistor current gain β and cut-off frequency f_T at low bias currents, the collector bias current of Q_1 is chosen to be 5 mA. At this off-optimum bias point, the amplifier noise level is increased by less than 0.4 dB, which corresponds to only 0.2 dB in receiver sensitivity for the p-i-n photodiode. The collector bias current of the second stage transistor Q_2 is chosen to be 10 mA to provide a good dynamic swing into the 50 ohm load.

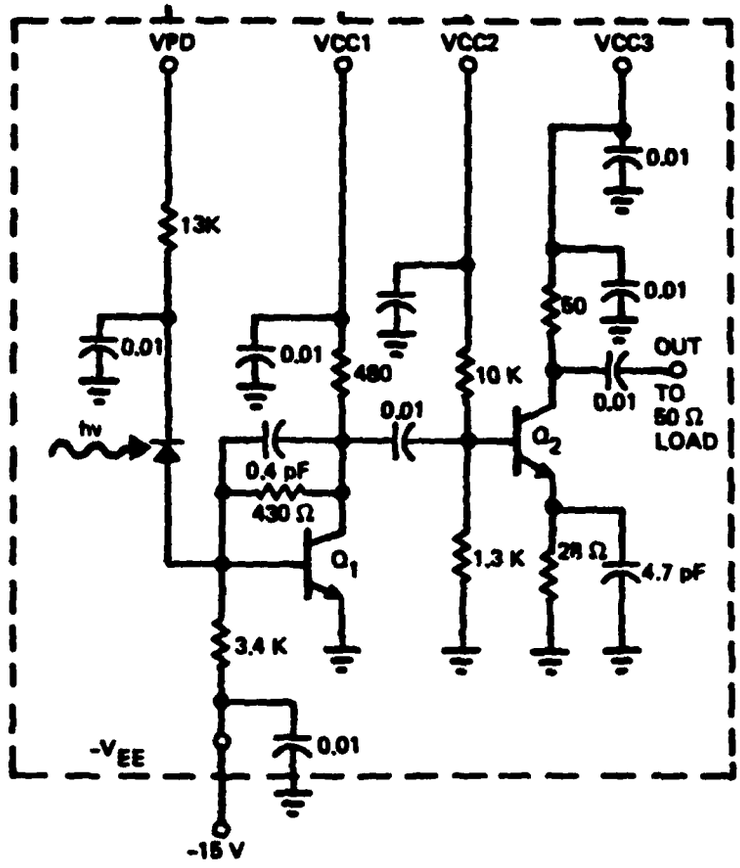

Figure 1. Schematic of 1.3 μm optical receiver.

2.2 Fabrication

The optical receiver amplifier is fabricated using thin film hybrid circuit construction. The hybrid circuit layout is shown in Figure 2 where the circuit elements are identified. Interdigitated capacitances are used for C_F and C_E so that their values can be trimmed simply by breaking up or making wire bonds between various conductor pads. Similarly, trimming provisions are also provided for the collector and emitter resistance of the second stage to avoid the laser trimming process. These trimming provisions are incorporated at the initial layout in order to facilitate component value adjustment. However, it is found out by later measurements that the amplifier performance is relatively insensitive to their values.

Two prototypes of the optical receiver amplifier are fabricated. They will be referred to as prototype A and B. Both prototypes are mounted on standard 24 pin dual-in-line package (DIP) carriers. A photograph of the fabricated hybrid receiver prototype is shown in Figure 3. The 1.3 μm p-i-n photodiode (C30979 from RCA) can be seen at the left bottom corner of the package.

The hybrid optical receiver prototype is mounted on a test circuit board to provide biasing and output signal connection. The schematic diagram of receiver prototype A (within dashed box) and the test circuit board together with circuit elements values is shown in Figure 4.

2.3 Experimental Results

The frequency response of the optical receiver is measured on an optical network analyzer. A block diagram of the measurement set up is shown in Figure 5. It is based on an electrical network analyzer (HP 8505A) with the addition of an optical source and a reference optical detector. The optical source used is a 1.3 μm fiber-pigtailed buried-heterostructure laser (HLP 5500 from Hitachi). The frequency of the modulation is swept from 10 KHz to 1.3 GHz. The laser fiber pigtail is focussed on the optical receiver prototype under test. The laser backface optical power is focussed on a reference 1.3 μm p-i-n photodiode. This reference p-i-n detector is loaded

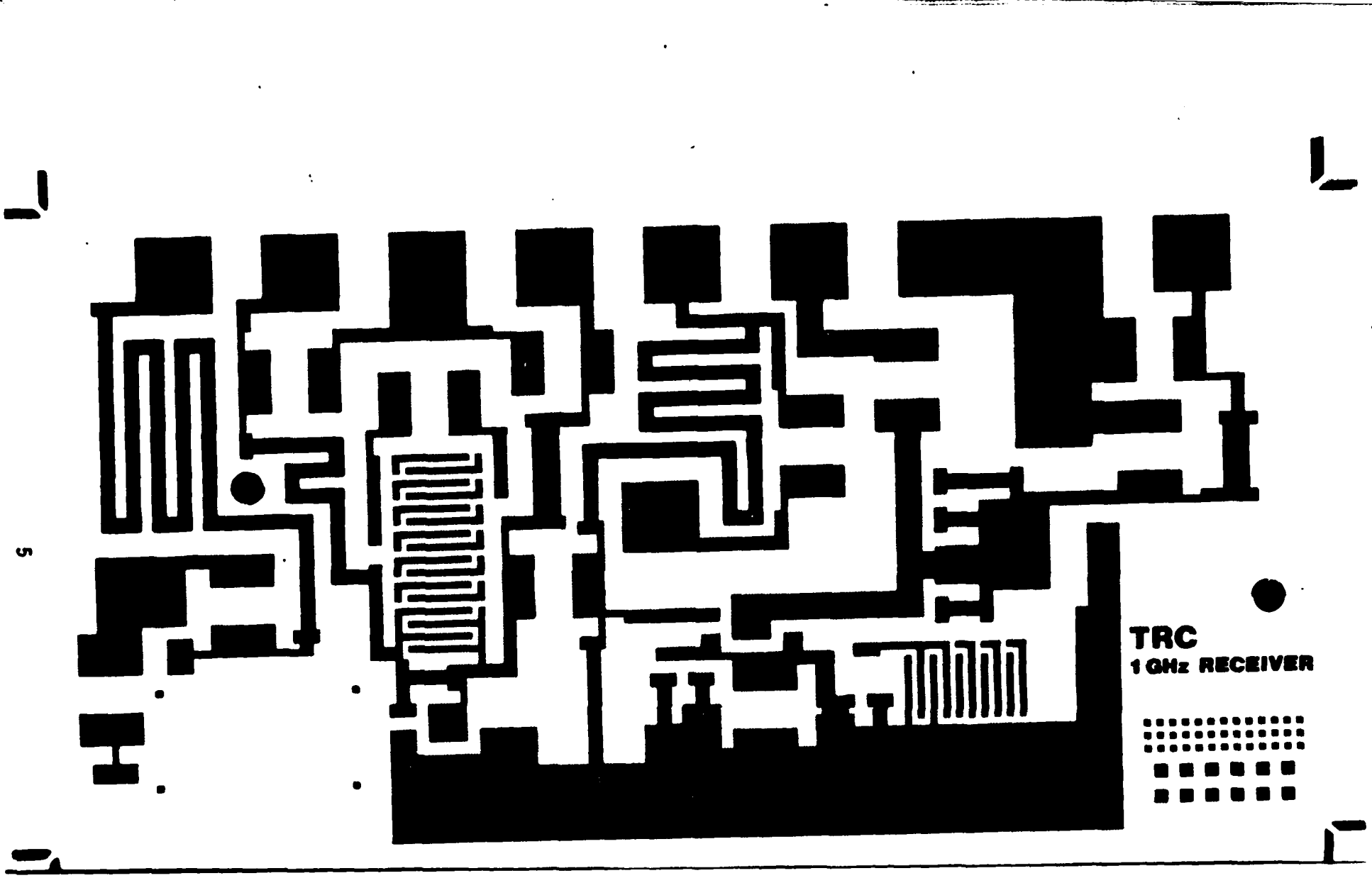

Figure 2. Thin film hybrid circuit layout of 1.3 μm optical receiver.

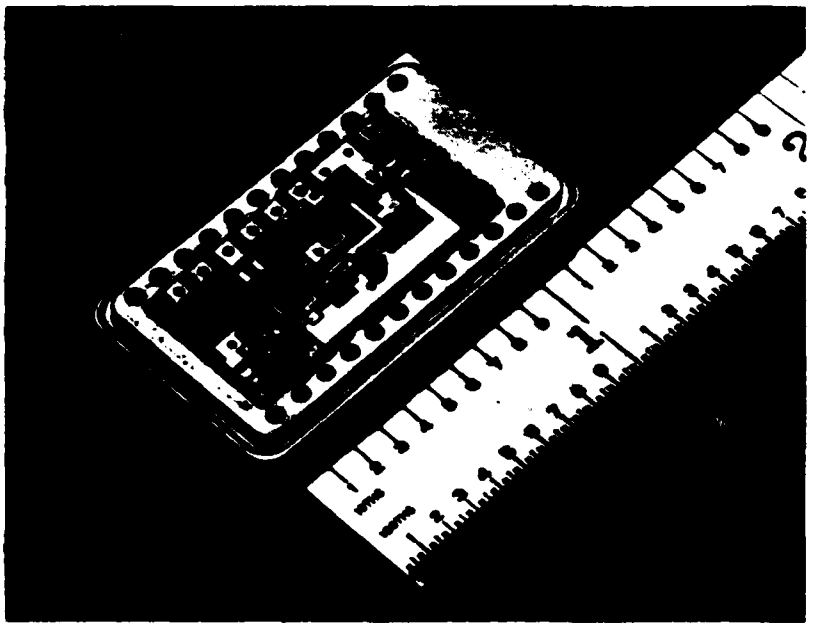

Figure 3. Photograph of 1.3 μm optical receiver prototype.

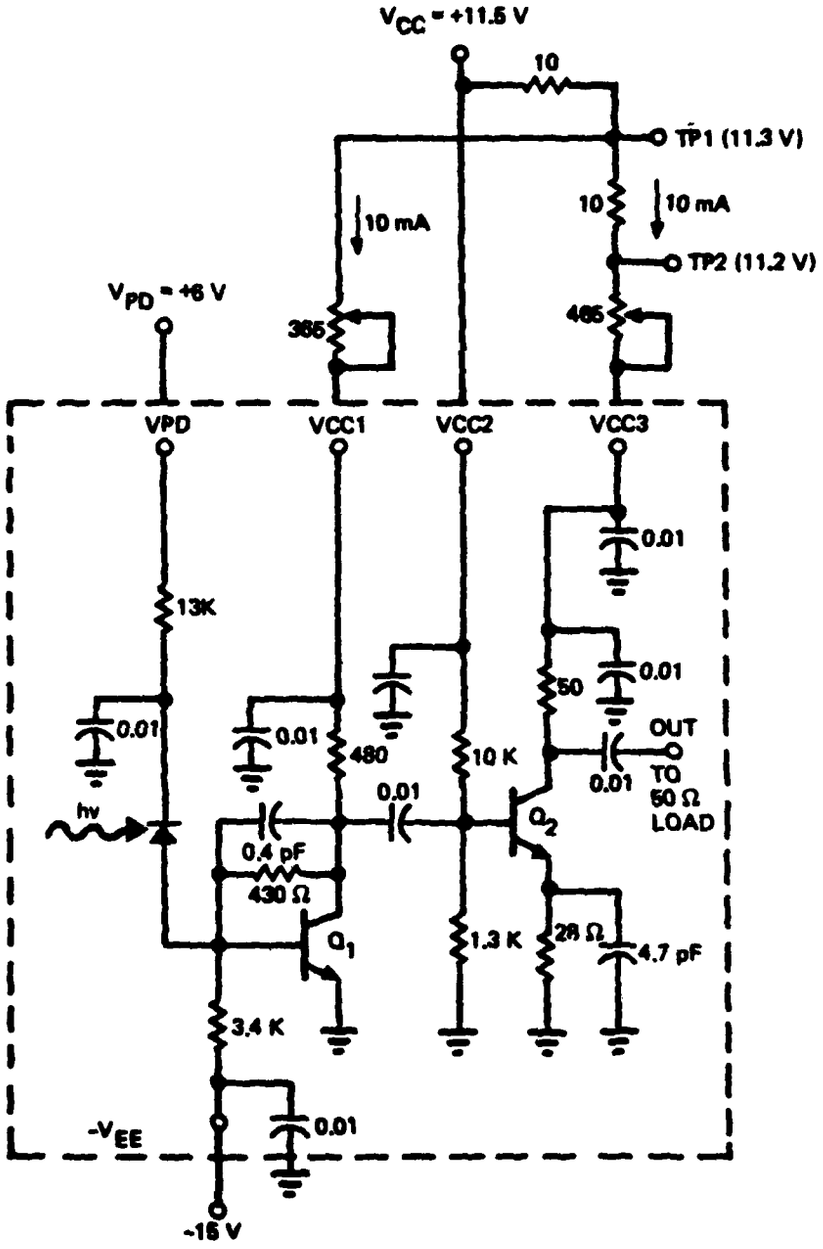

Figure 4. Prototype A schematic diagram.

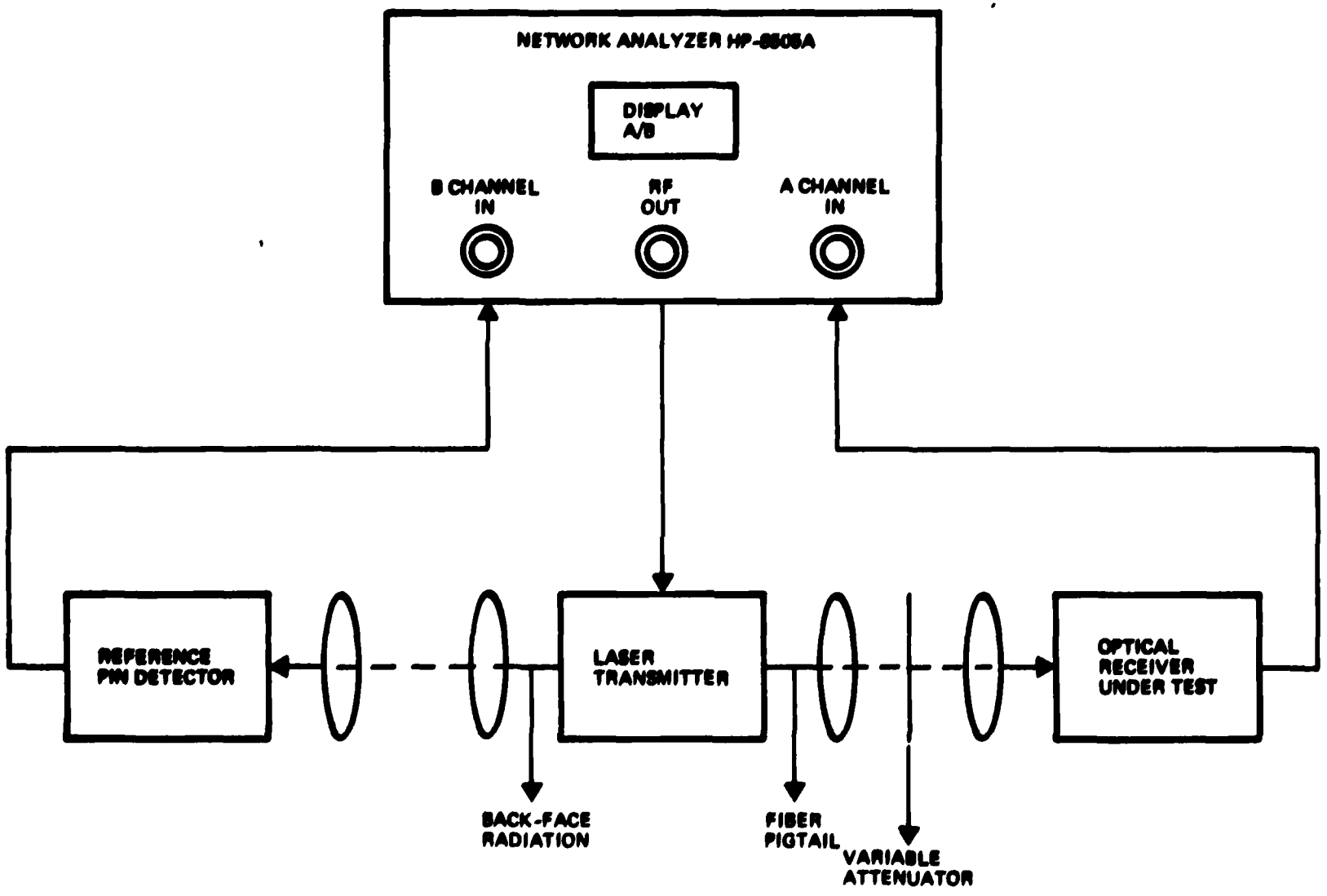

Figure 5. Optical network analyzer set up (up to 1.3 GHz).

into 50 ohm to provide a wide bandwidth. Thus the reference p-i-n diode response is a measure of the laser transmitter frequency response. Therefore, the frequency response of the optical receiver under test can be derived by dividing the optical receiver output with the reference p-i-n detector output. This division (or substraction on a dB scale) is done automatically by the network analyzer. A picture of the measurement set-up is shown in Figure 6.

The frequency response of the optical receiver prototype A is shown in Figure 7. It can be seen that the amplitude response is flat to ±0.25 dB and the phase response is linear to ±2.5 ° over the whole frequency band (up to 1.3 GHz). A significant contribution to the ripples seen on the amplitude and phase response is due to reflections and cross coupling of coaxial RF cables because the ripple positions are different for different cable lengths. Thus the intrinsic ripple of the optical receiver is in fact better than observed on the network analyzer.

Another plot of the amplitude response of receiver prototype A with frequency is shown in Figure 8. In this case, the reference p-i-n detector is an ultra fast p-i-n detector (QD-100-UHS from Lasertron) with a bandwidth exceeding 6 GHz. The measured frequency response is slightly flatter than in Figure 7 because of a better measurement set up.

Since the optical receiver is essentially flat up to the high frequency limit of this optical network analyzer set up (1.3 GHz), another measurement set up is necessary to determine its bandwidth. This test set up as shown in Figure 9 consists of a frequency synthesizer (HP 8662A) used as a sweep generator and a spectrum analyzer (HP 8566A). The modulation frequency is swept from 100 MHz to 2.4 GHz while the spectrum analyzer is set for the 0 to 2.5 GHz band. The correction for the laser frequency response by the Lasertron reference p-i-n receiver is also obtained on the spectrum analyzer. The measured frequency response, shown in Figure 10, is thus the response of the optical receiver under test. It can be observed that the response is ± 0.5 dB flat to 2 GHz, with a 3 dB bandwidth of 2.2 GHz.

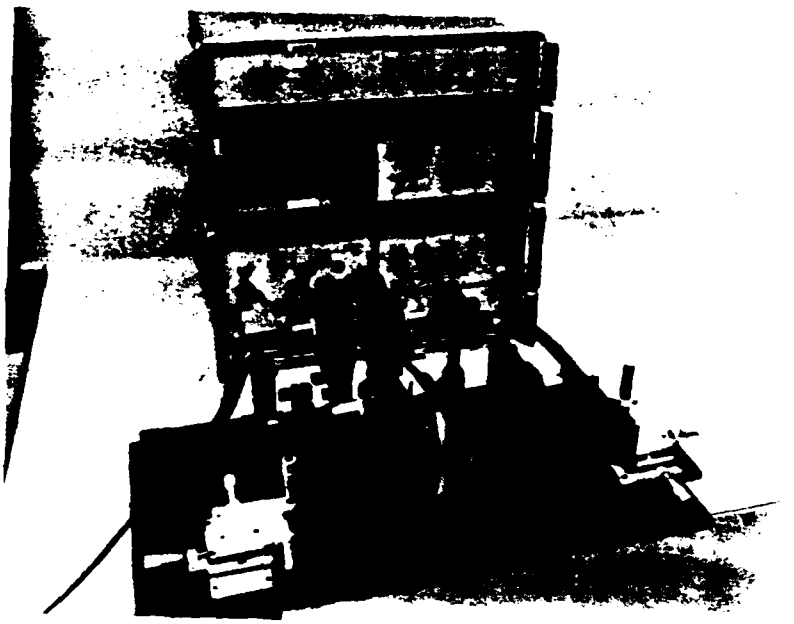

Figure 6. Photograph of the frequency response measurement set up.

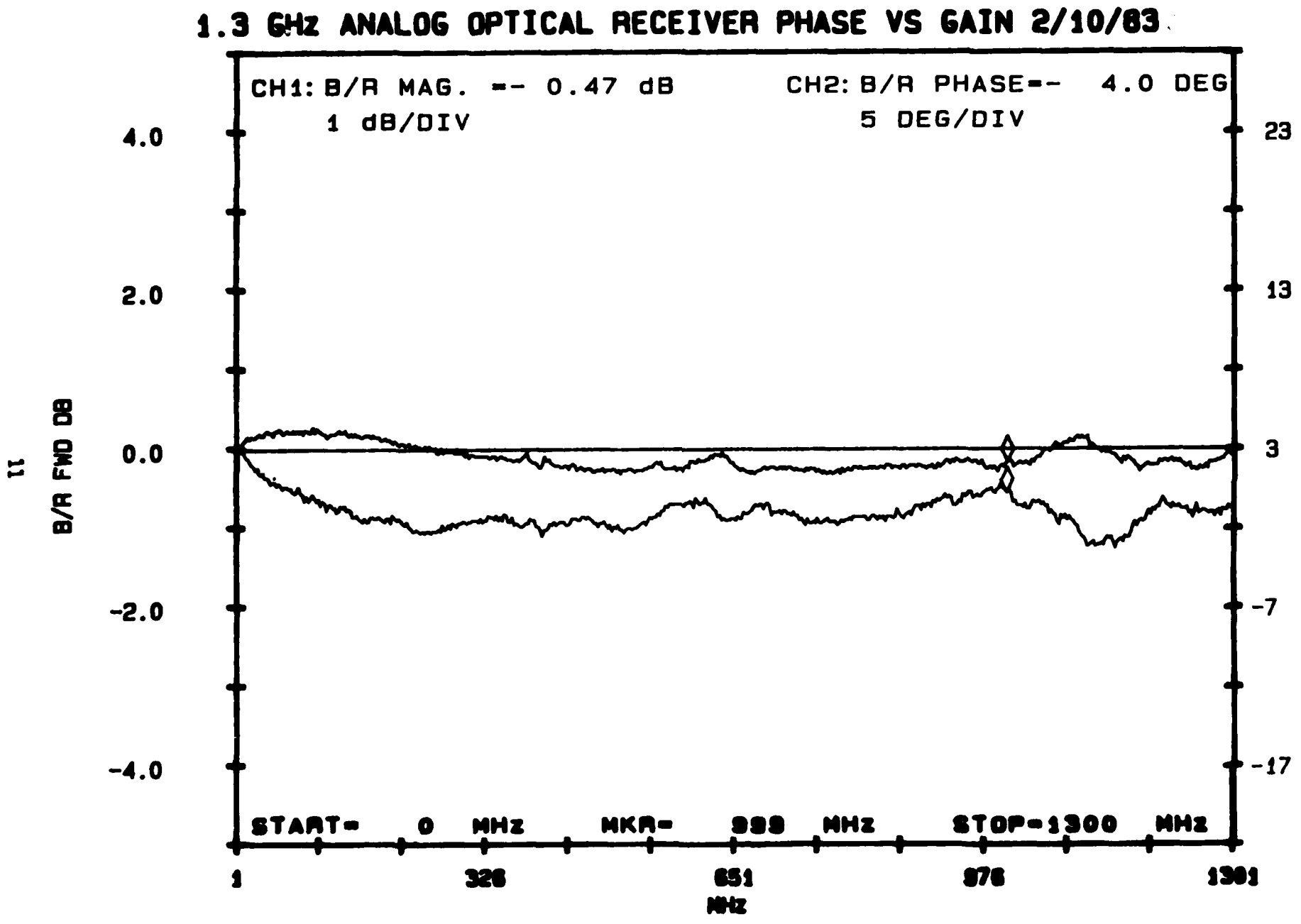

Figure 7. Amplitude and phase response of receiver prototype A using RCA p-i-n diode as reference detector.

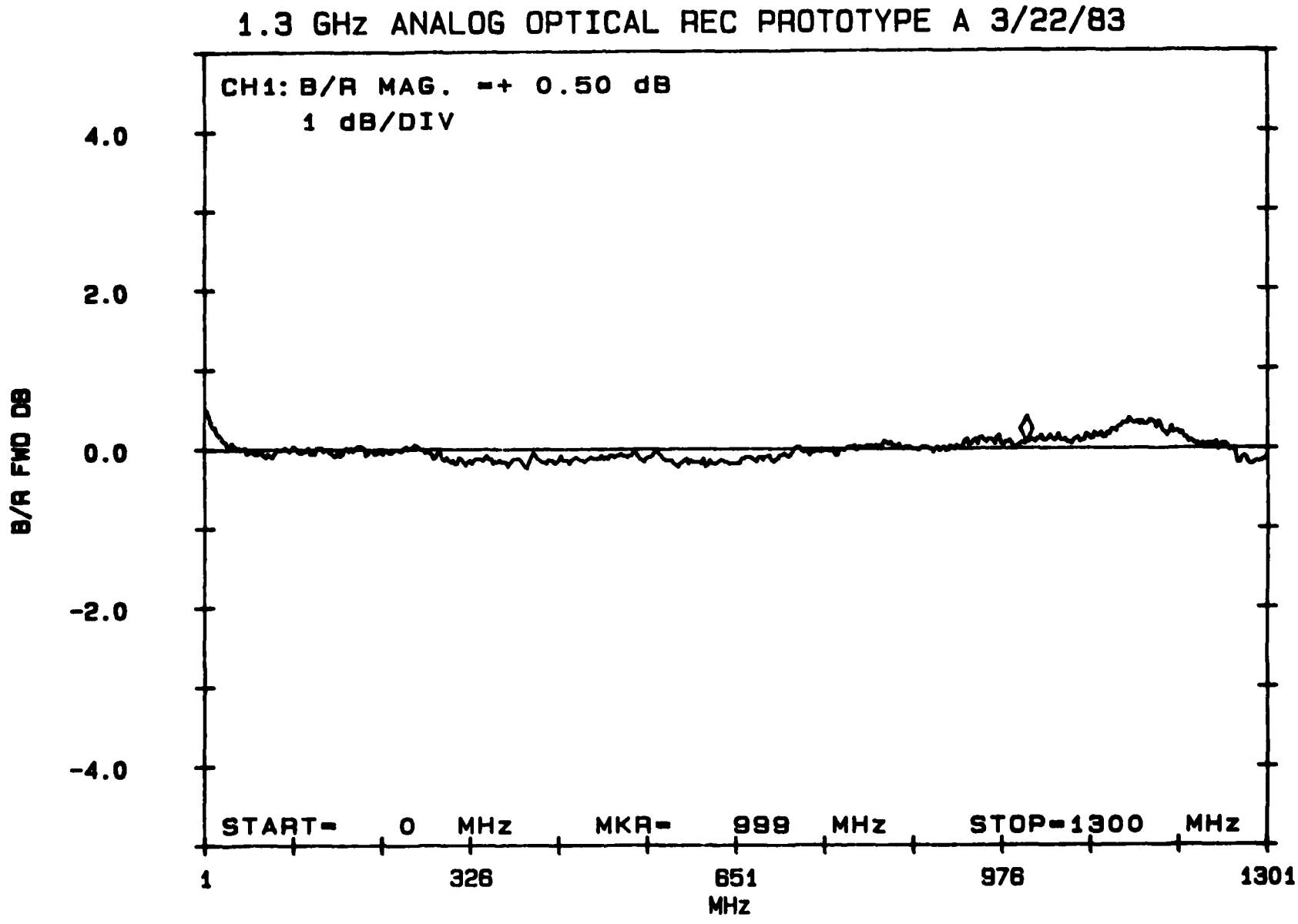

Figure 8. Frequency response of receiver prototype A using ultra fast Lasertron p-i-n diode as reference detector.

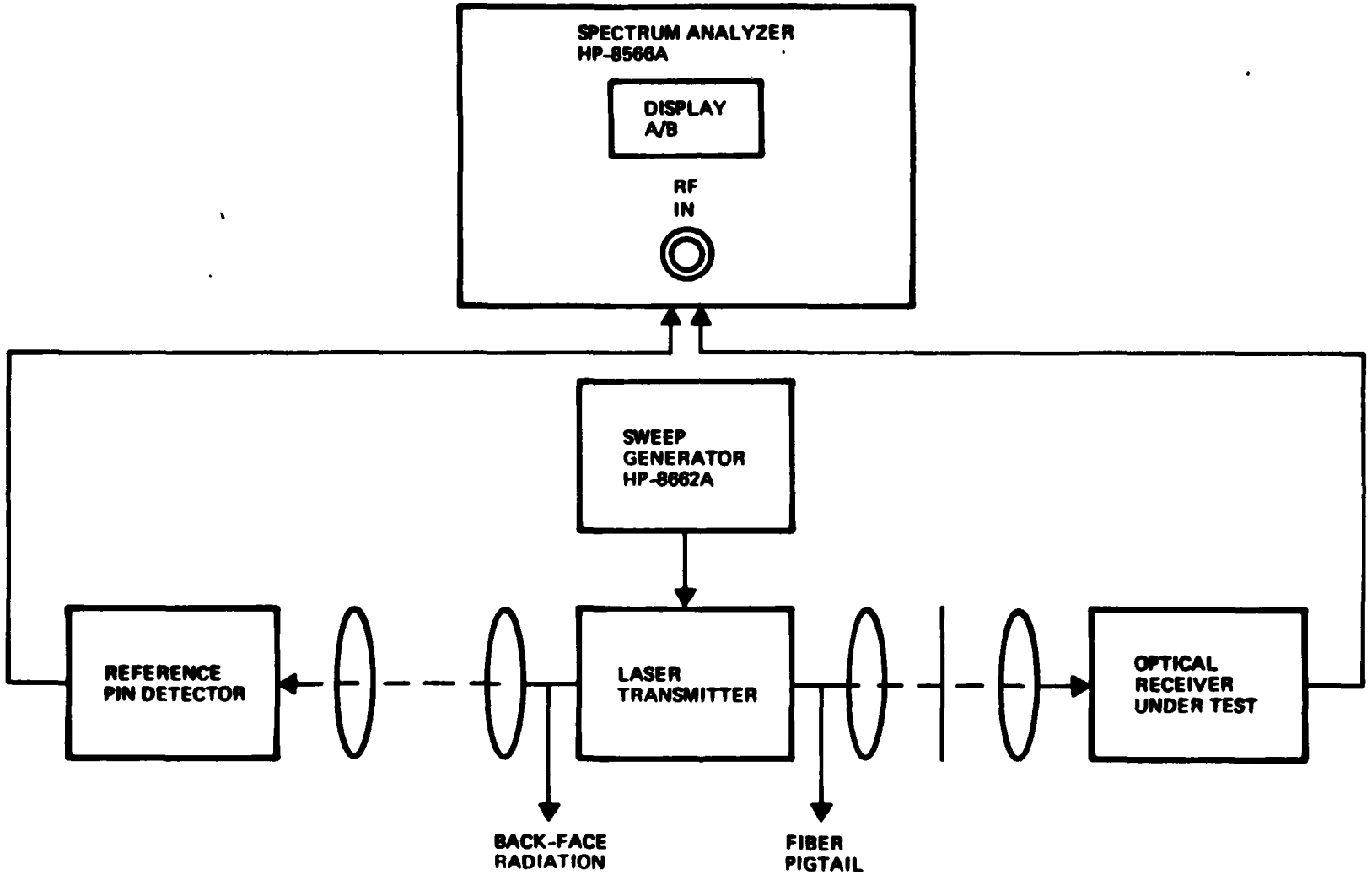

Figure 9. Measurement set up for frequency measurement up to 2.5 GHz.

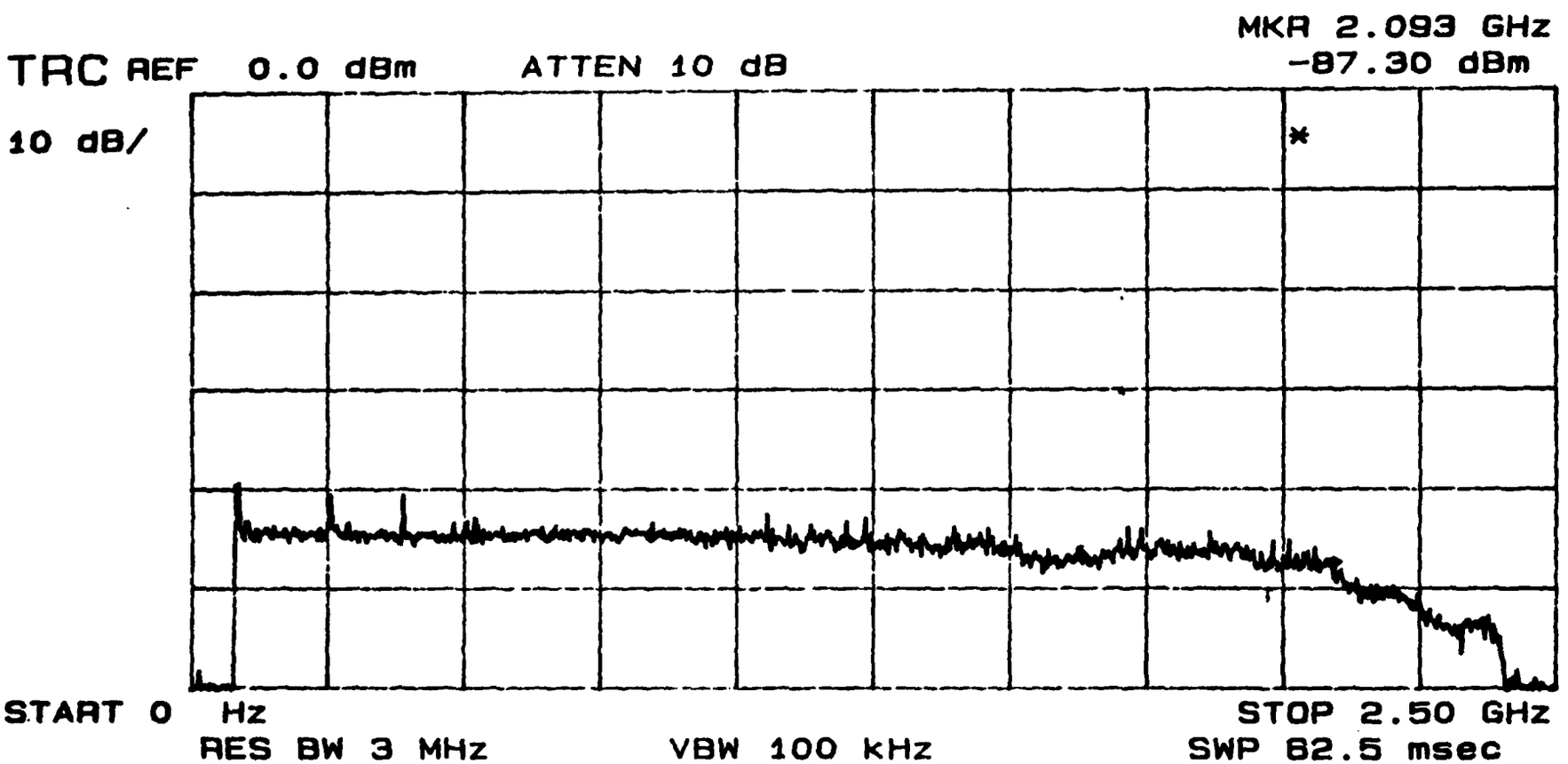

Figure 10. Frequency response of prototype A (measured up to 2.4 GHz).

The optical receiver noise performance has also been characterized on the spectrum analyzer. Since the receiver output noise is small, it needs to be amplified in order to be raised above the noise floor of the spectrum analyzer. A wideband 10 MHz - 1.3 GHz amplifier module (HP 10855A) with 26 dB gain is used to amplify the optical receiver noise output. The measured amplified noise spectrum is shown in Figure 11. The top trace is the receiver noise spectrum and the bottom trace is the noise floor of the HP amplifier module and the spectrum analyzer. It should be noted that the roll-off after 1.3 GHz is due to the HP amplifier module, as is also evident from the bottom trace. The optical receiver optical output noise power can thus be evaluated. Thus, the input equivalent noise current spectral density can be determined by dividing by the transimpedance of the optical receiver.

The transimpedance of the receiver prototype A was measured to be 280 Ω , in good agreement with computer simulation. The quantum efficiency of the p-i-n photodiode is approximately 60%, corresponding to a responsitivity of 0.6 A/W. Thus the total responsitivity of the optical receiver is approximately 168 volt/watt. The transimpedance is chosen to be 280 Ω nominal for the simplicity of the optical receiver design. Its value can be increased simply by following the optical receiver with a gain block. This "gain block" is a standard microwave amplifier and can be readily designed or obtained commercially.

The input equivalent noise current spectral density calculated from the results in Figure 11 is plotted in Figure 12 together with results predicted from theory and computer simulation (SPICE program). The input equivalent noise current spectral density due to the first amplifier stage is given by [1, 2]:

$$N(f) = \frac{4kT}{R_F} + 2eI_b + \frac{2e}{I_c}(2\pi V_T C_T)^2 f^2 + 4kTr_{bb'}(2\pi C_{dsf})^2 f^2 \qquad (1)$$

where R_F is the parallel combination of the feedback resistance and the base bias resistance of the first stage.

I_b and I_c are the base and collector bias current of Q_1

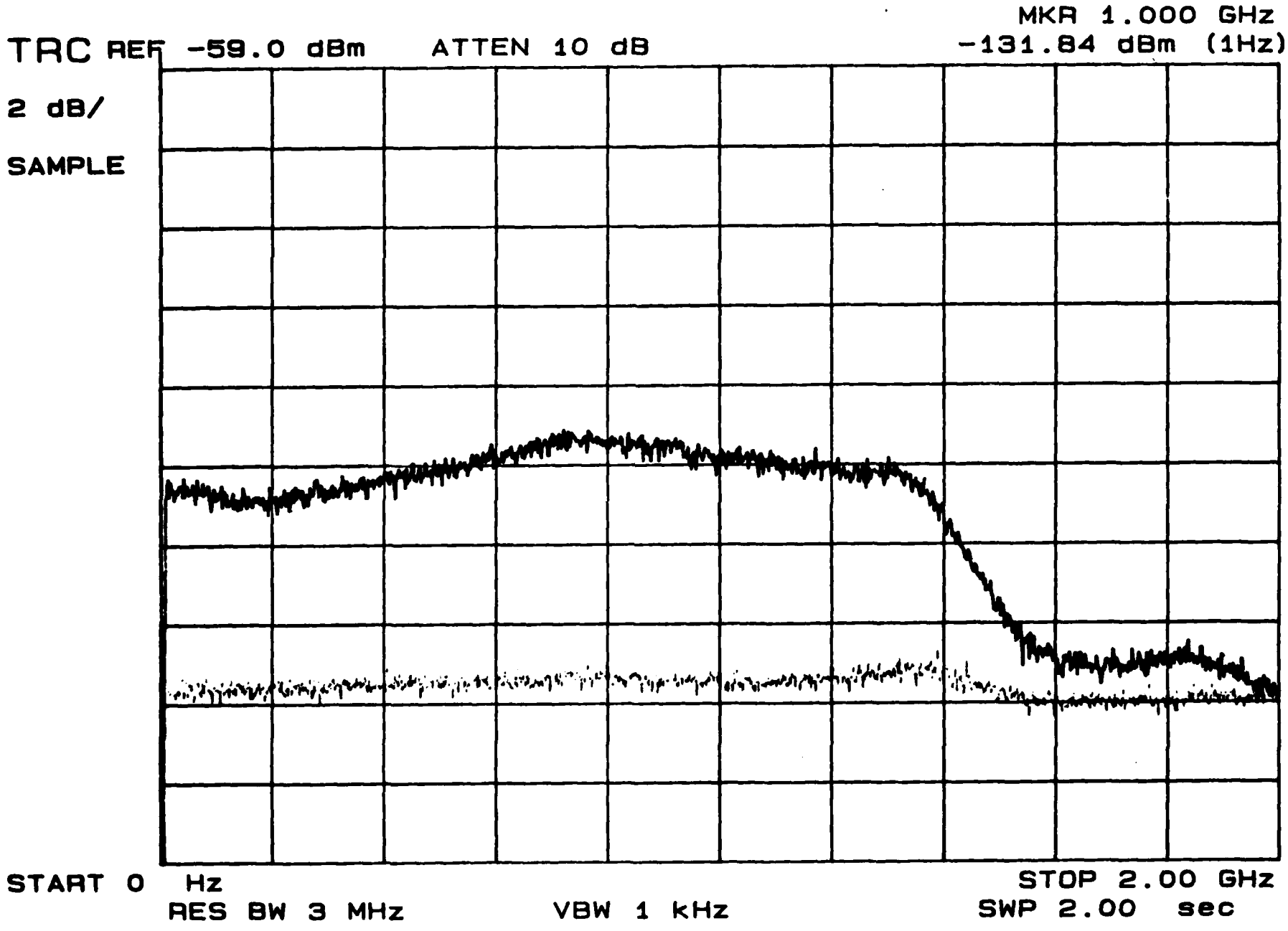

Figure 11. Measured noise spectrum of prototype A followed by a 10 MHz-1.3 GHz amplifier module with 26 dB gain.

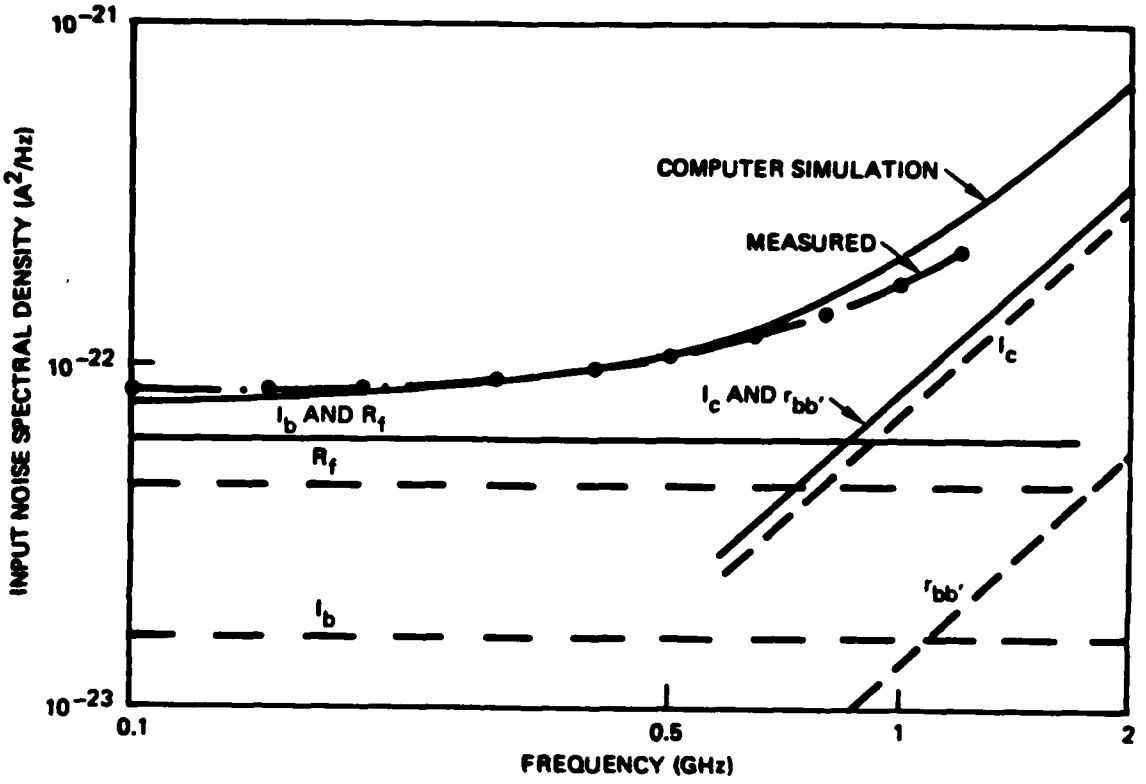

Figure 12. Input equivalent noise spectral density of prototype A.

$r_{bb'}$ is the base spreading resistance of Q_1

C_T is the total input capacitance

C_{dsf} is the sum of the detector, stray capacitance and the feedback capacitance.

k is the Boltzmann constant

T is the absolute temperature

e is the change of an electron

and V_T is a constant given by:

$$V_T = kT/e \tag{2}$$

The first term in equation (1) is due to the thermal noise of the feedback resistance and base bias resistance. The second term is due to the shot noise of the base current. Both these noise contributions are flat with frequency. The third and fourth terms which are due to the collector shot noise and the base spreading resistor thermal noise, increases with frequency as f^2. All four components are shown in Figure 12.

The input equivalent noise current spectral density of the complete receiver amplifier as simulated by SPICE program is shown as the solid curve. It is slightly higher than the sum of the four components above because of noise contribution from the second stage.

The measured input equivalent noise is shown in Figure 12 as a dotted line. It can be observed that the experimental results agree well with the predicted values. The input equivalent noise spectral density is $9pA/\sqrt{Hz}$ with a 3 dB noise corner frequency of approximately 920 MHz. The input noise power averaged over the 0 to 1 GHz band can therefore be evaluated to be 1.13×10^{-13} A^2. This corresponds to an input equivalent noise resistance of 146 ohm. The noise level achieved is 1.6 dB bettern than the required

specification of 100 ohm equivalent noise resistance.

The optical receiver performance thus exceeds the required specifications in both frequency response and noise performance.

The measured output reflection coefficient s_{22} of receiver prototype A is shown in Figure 13. It can be observed that the reflection increases at high frequencies. At 1 GHz we have:

$$|S_{22}| = -12.3 \text{ dB} = 0.242$$

The corresponding voltage standing wave ratio (VSWR) is:

$$\text{VSWR} = \frac{1 + |S_{22}|}{1 - |S_{22}|} = 1.64$$

Thus over the 0 to 1 GHz frequency band, the worst case VSWR ratio is 1.64.

The receiver prototype B has also been fully characterized under the same test set-up. This prototype is chosen from a substrate with a different resistivity. The corresponding circuit component values are shown in Figure 14. Therefore, this prototype can be used to check the design sensitivity of component tolerances.

Essentially, the same performance as with prototype A is obtained. The frequency response of prototype B obtained on the optical network analyzer is shown in Figure 15. The output noise spectrum after amplification by the HP amplifier module is shown in Figure 16. Again, the frequency roll-off after 1.3 GHz is due to the HP amplifier. Both plots are identical to those of prototype A.

The measured output reflection coefficient s_{22} of receiver prototype B is shown in Figure 17. Again, it can be observed that the reflection increases with frequencies. At 1.3 GHz we obtain:

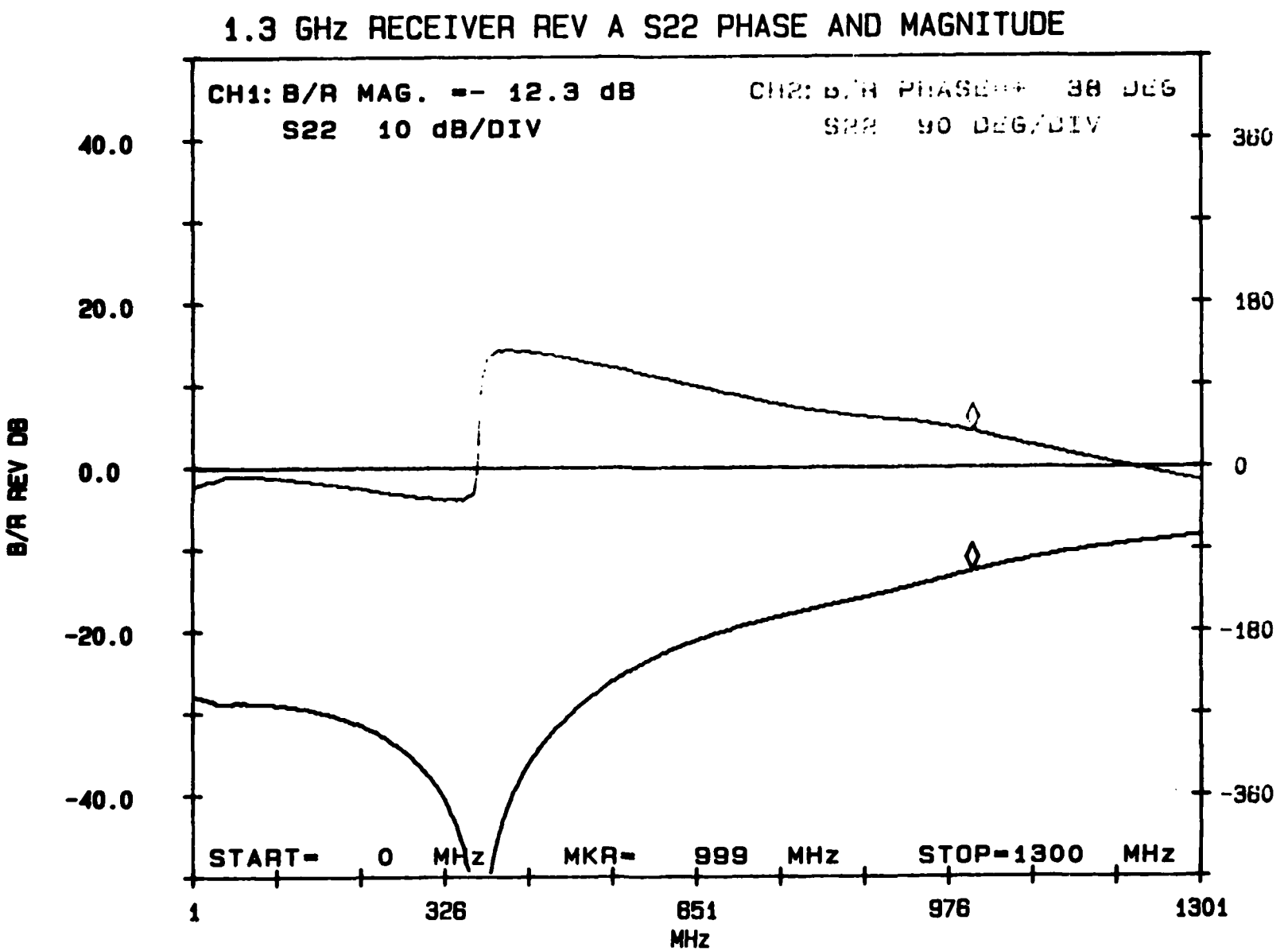

Figure 13. Output reflection coefficient s_{22} of prototype A.

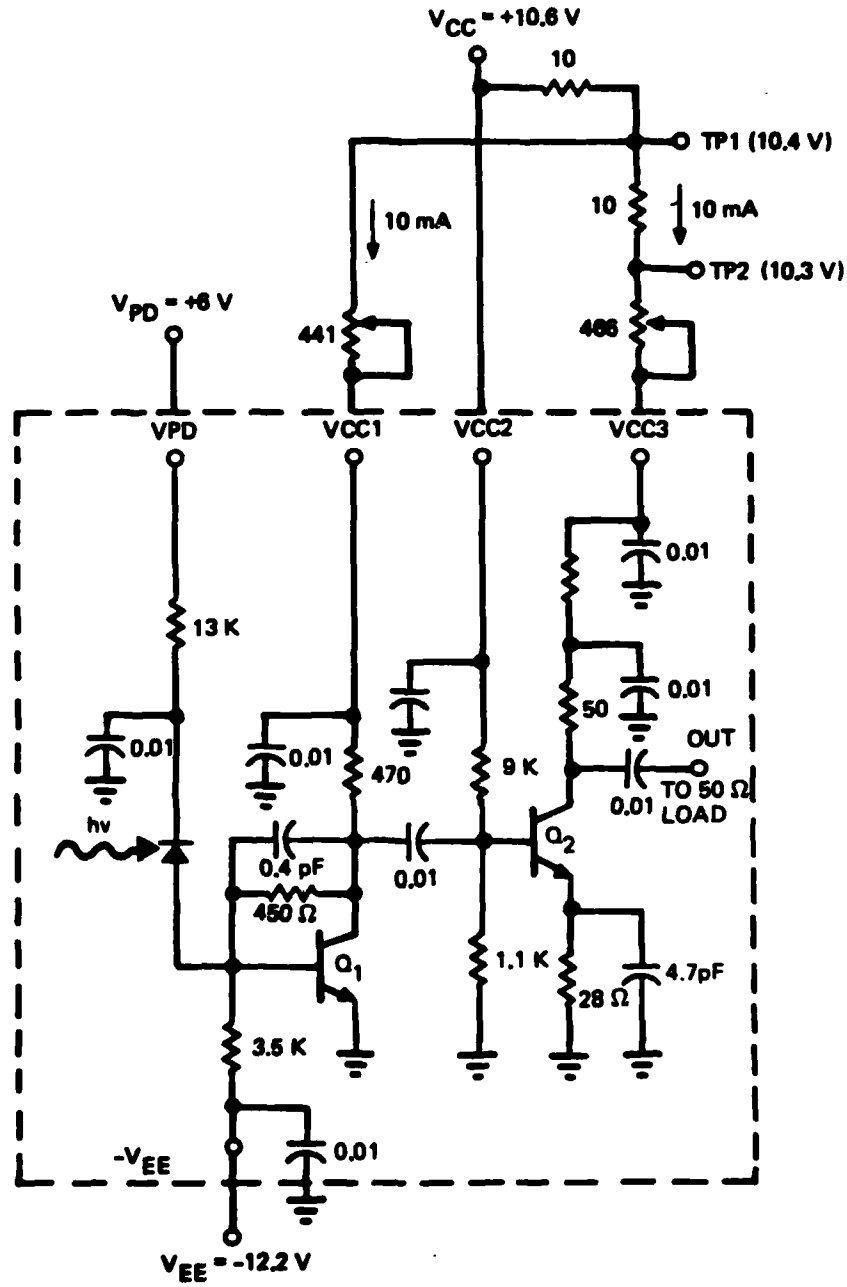

Figure 14. Prototype B schematic diagram.

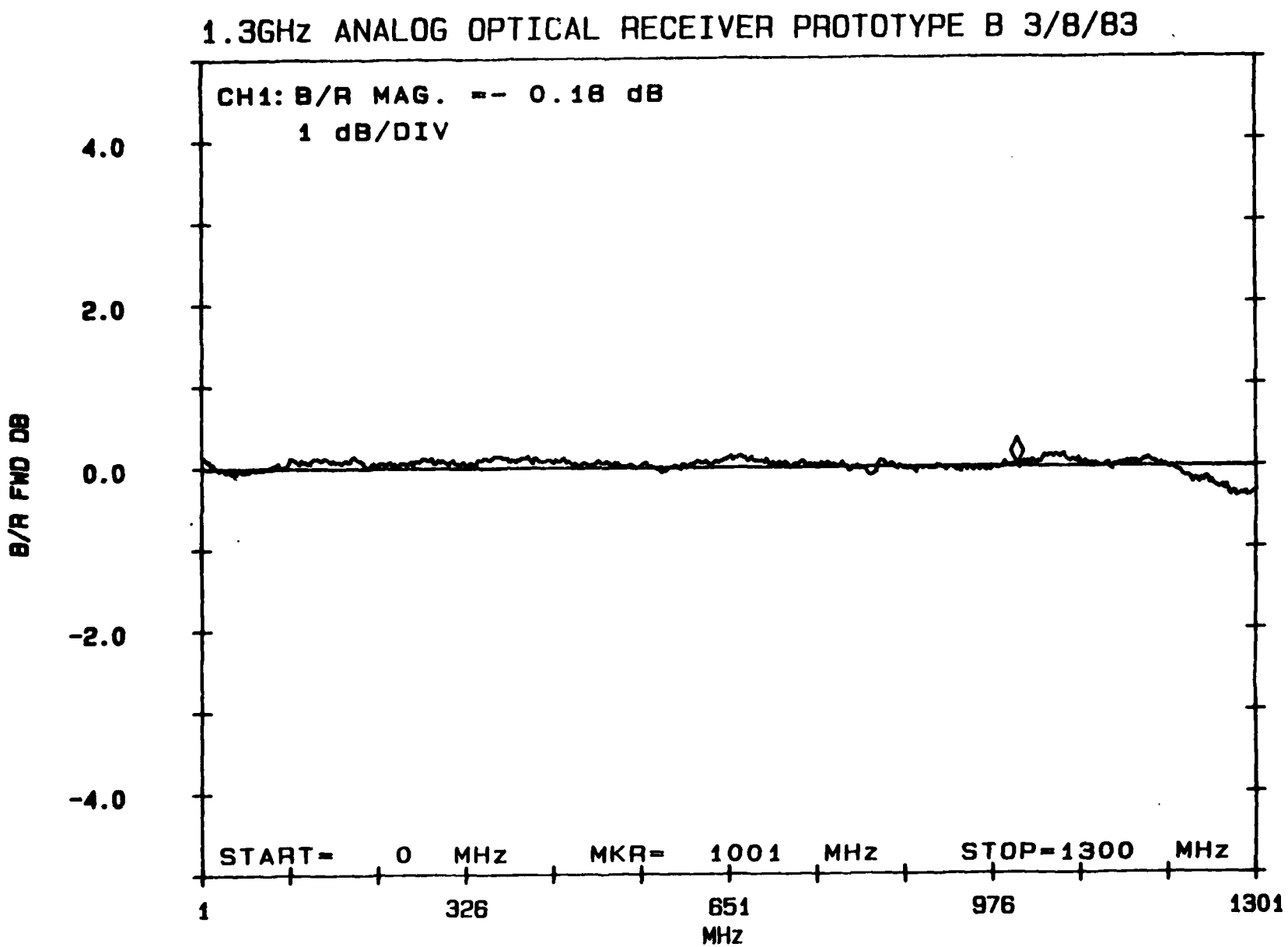

Figure 15. Frequency response of prototype B.

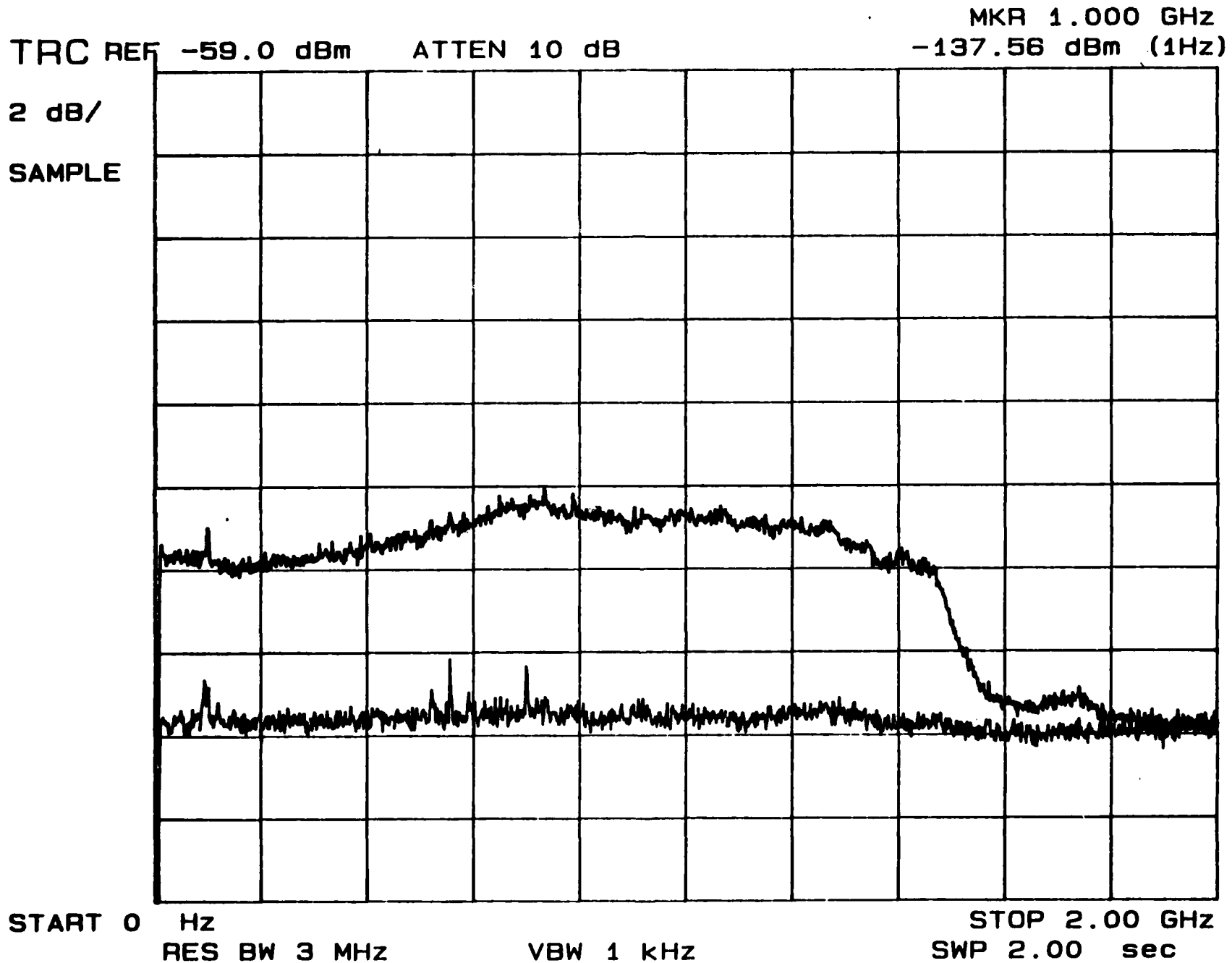

Figure 16. Output noise spectrum of prototype B after amplification by HP amplifier module.

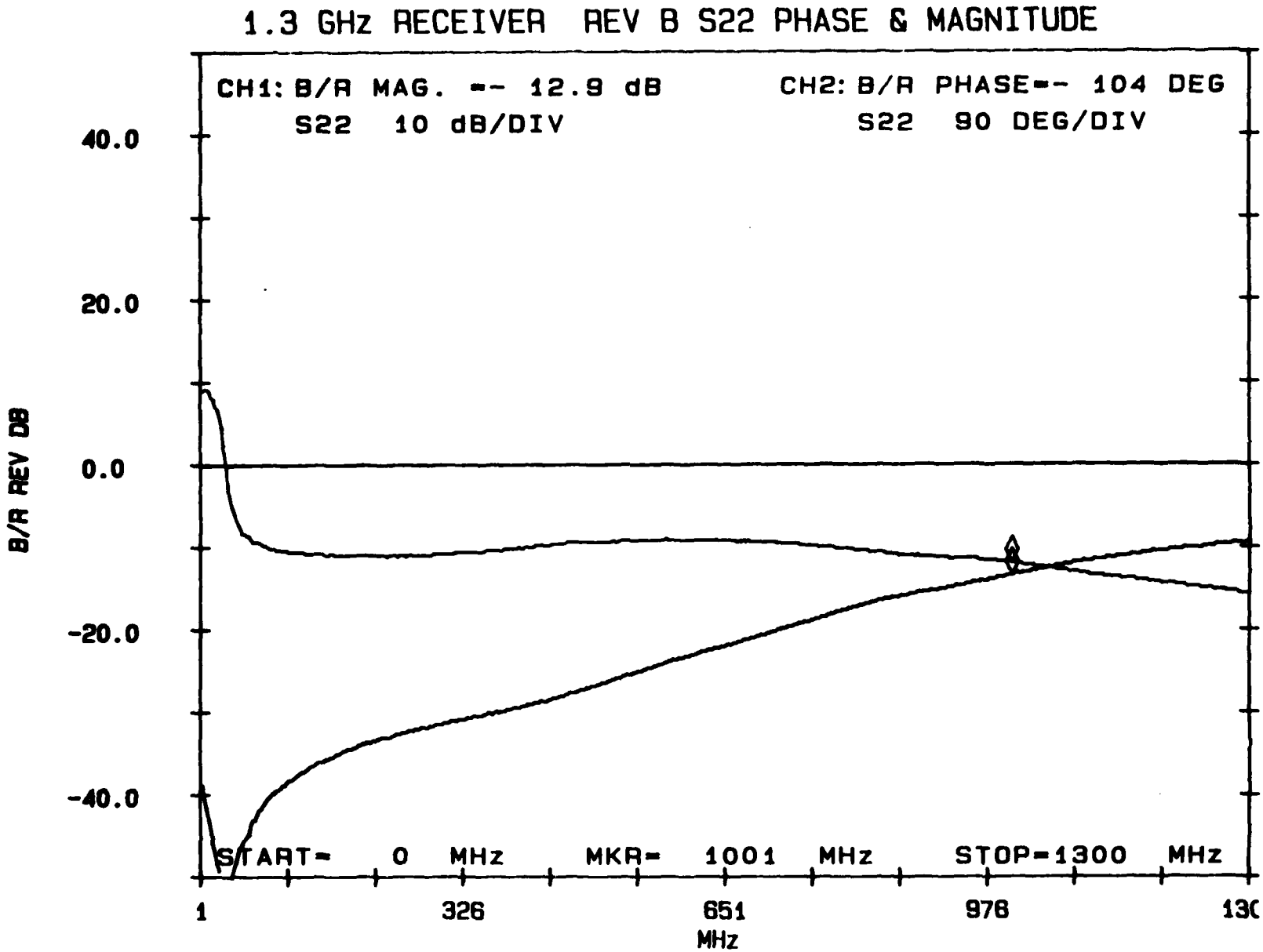

Figure 17. Output reflection coefficient s_{22} of prototype B.

$$|S_{22}| = -12.9 \text{ dB} = 0.226$$

corresponding to a VSWR of

$$\text{VSWR} = \frac{1 + |S_{22}|}{1 - |S_{22}|} = 1.58$$

Thus, in summary, the 1.3 μm optical receiver has been designed and fully tested. The experimental results of the two prototypes fabricated are essentially the same and in agreement with performances predicted from theory and computer simulation. The optical receiver frequency response is flat to ± 0.5 dB up to 2 GHz with a 3 dB bandwidth of 2.2 GHz. It is flat to ±0.25 dB over the 0 to 1.3 GHz frequency band. In addition to this excellent frequency response, it also possesses really low noise performance. The input equivalent noise spectral density achieved is $9\text{pA}/\sqrt{\text{Hz}}$ with a 3 dB corner frequency of 920 MHz. This corresponds to an input equivalent noise resistance of 146 ohms. Both noise level and bandwidth capability exceed design goals.

3. 1 GHz RECIRCULATING DELAY LINE SYSTEM ANALYSIS

3.1 System Analysis and Performance

The preliminary system analysis of the Recirculating Delay Line was carried out in the previous phase (contract number N00014-81-C-2412, "1 GHz Bandwidth Recirculating Optical Analog Repeater"). In this report, we will refine and extend the previous analysis and derive the specifications for the necessary component requirements.

A block diagram of the recirculating delay line is shown in Figure 18. It consists of 4 main components: an optical transmitter, a transmission single mode fiber as the optical delay line, an optical receiver, and an "interface amplifier" for input/output connection.

The input to the delay line is referred to as the "broadband access port". An electrical signal injected to this port modulates the optical transmitter which incorporates an injection laser diode. The optical transmitter output is coupled into the delay fiber, which is chosen to be single mode for minimum dispersion. The operating wavelength is chosen to be in the long wavelength region, either 1.3 μm or 1.55 μm for minimum fiber loss. The signal at the fiber output thus delayed by the fiber propagation time T_f. This signal is then detected by the optical receiver, amplified by the interface amplifier and is fed back to the optical transmitter. The signal is thus recirculated around the loop. After the desired times of circulation, the delayed signal can be obtained at the "broadband monitor port". The total delay time is therefore given by $T_d = nT_f$ where n is the number of circulations around the loop. A "loss insertion control" is also provided which can be used (under automatic control) to break up the loop by increasing the loop loss by 10 dB or more when necessary.

The signal-to-noise ratio (SNR) of the signal detected at the optical receiver after the first pass through the fiber is referred to as the initial SNR. The initial SNR is a function of the optical power incident on the receiver, the receiver amplifier noise level and the initial modulation index. Since the recirculating loop gain has to be less than unity for

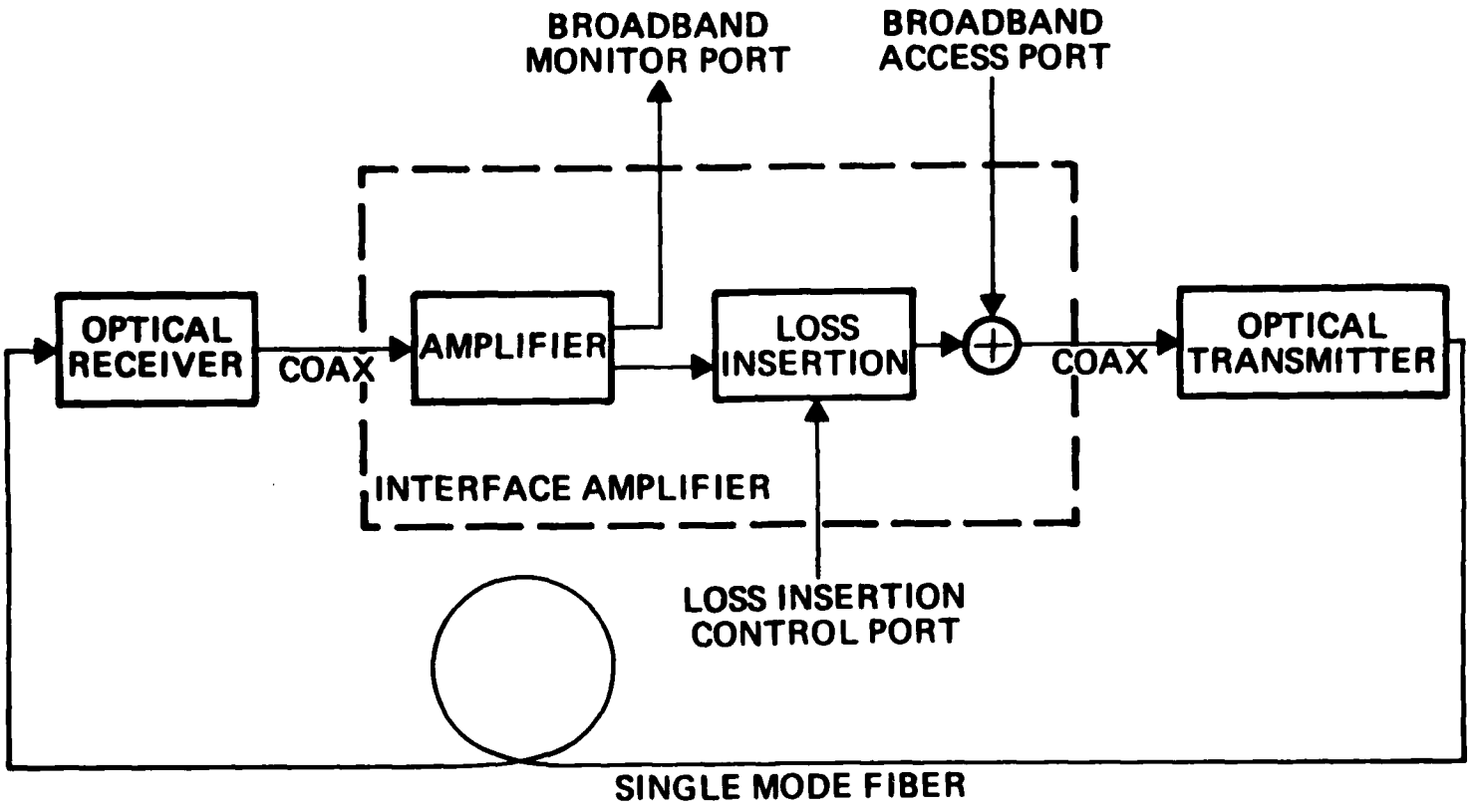

Figure 18. Recirculating delay line block diagram.

stability reasons, the modulation idex decreases as the signal propagates through the loop. Consequently, the SNR decreases because of this modulation index decrease and receiver amplifier noise. It can be shown that the SNR after n circulations through the loop, denoted by $(SNR)_n$ is related to the initial SNR denoted by $(SNR)_1$ by:

$$\frac{(SNR)_n}{(SNR)_1} = \frac{\beta^{-2} - 1}{\beta^{-2n} - 1}$$

where β is the loop gain ($\beta < 1$).

This SNR degradation is plotted in Figure 19 versus the loop loss for up to 10 circulations around the loop. It can be seen that a small value of loop loss is desirable to minimize the SNR degradation. However, the loop loss should have enough margin to allow for variation in the amplifier gain and the optical device transfer characteristics. From Figure 19, a loop loss value of 1 dB is the best compromise.

Signal distortion in the recirculating delay line is caused mainly by the laser diode nonlinearity. The degradation of second harmonic distortion and third harmonic distortion as the signal circulates through the loop has been evaluated. The distortion degradations are plotted in Figures 20 and 21 as a function of the loop loss for up to 10 circulations through the loop. It can be observed that as far as distortion is concerned, a high value of loop loss is desirable because this would result in a decreasing modulation index when the signal circulates through the loop. Since the laser nonlinearity decreases with modulation index, the distortion degradation is less for a higher value of loop loss.

Laser diode nonlinearity have been analyzed theoretically and measured experimentally[3]. To obtain good linearity, the laser has to be biased well above the threshold. The laser harmonic distortion increases with frequency and with modulation index. Typical second and third harmonic distortion for good quality laser diodes are:

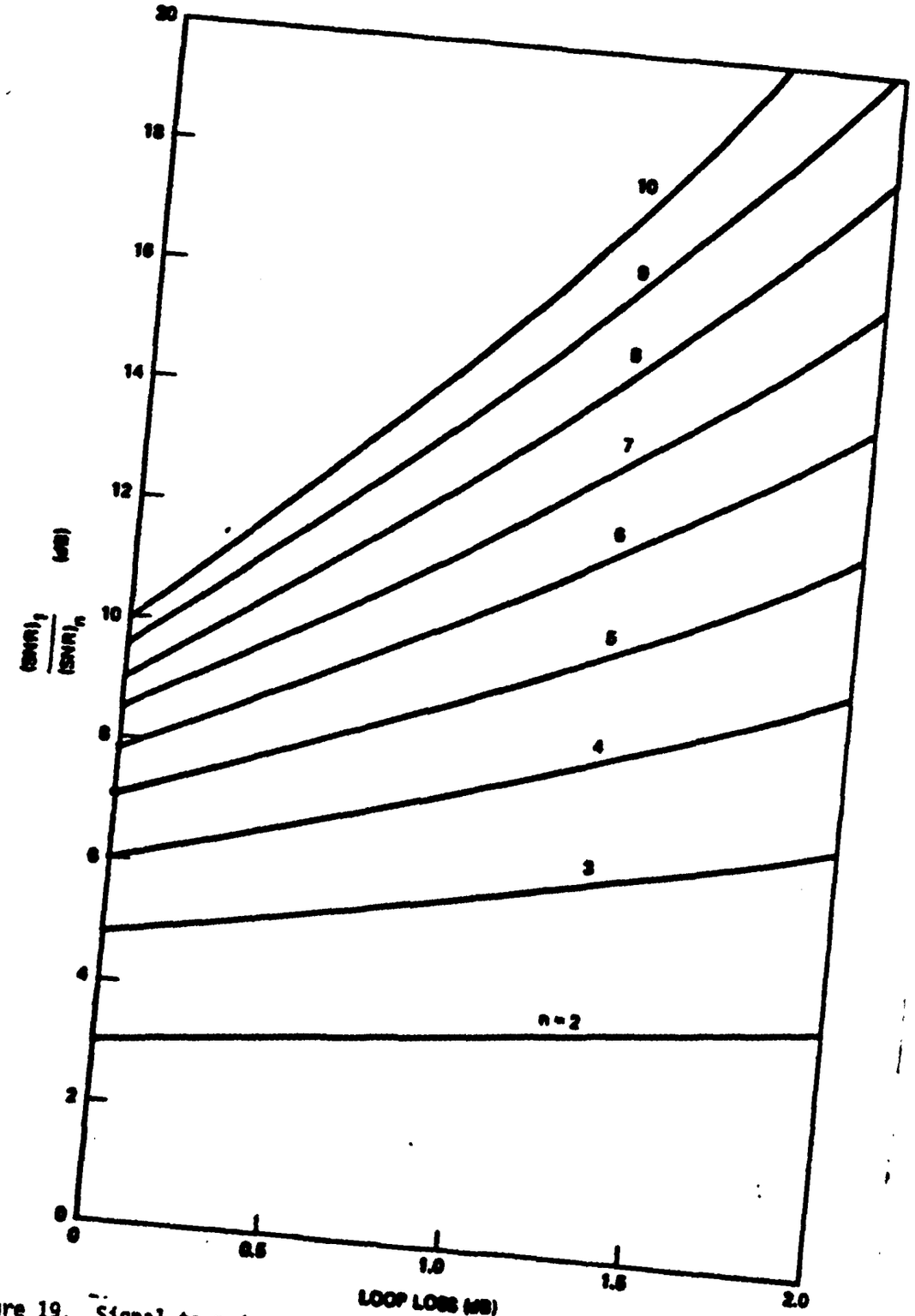

Figure 19. Signal-to-noise ratio degradation of recirculating delay line.

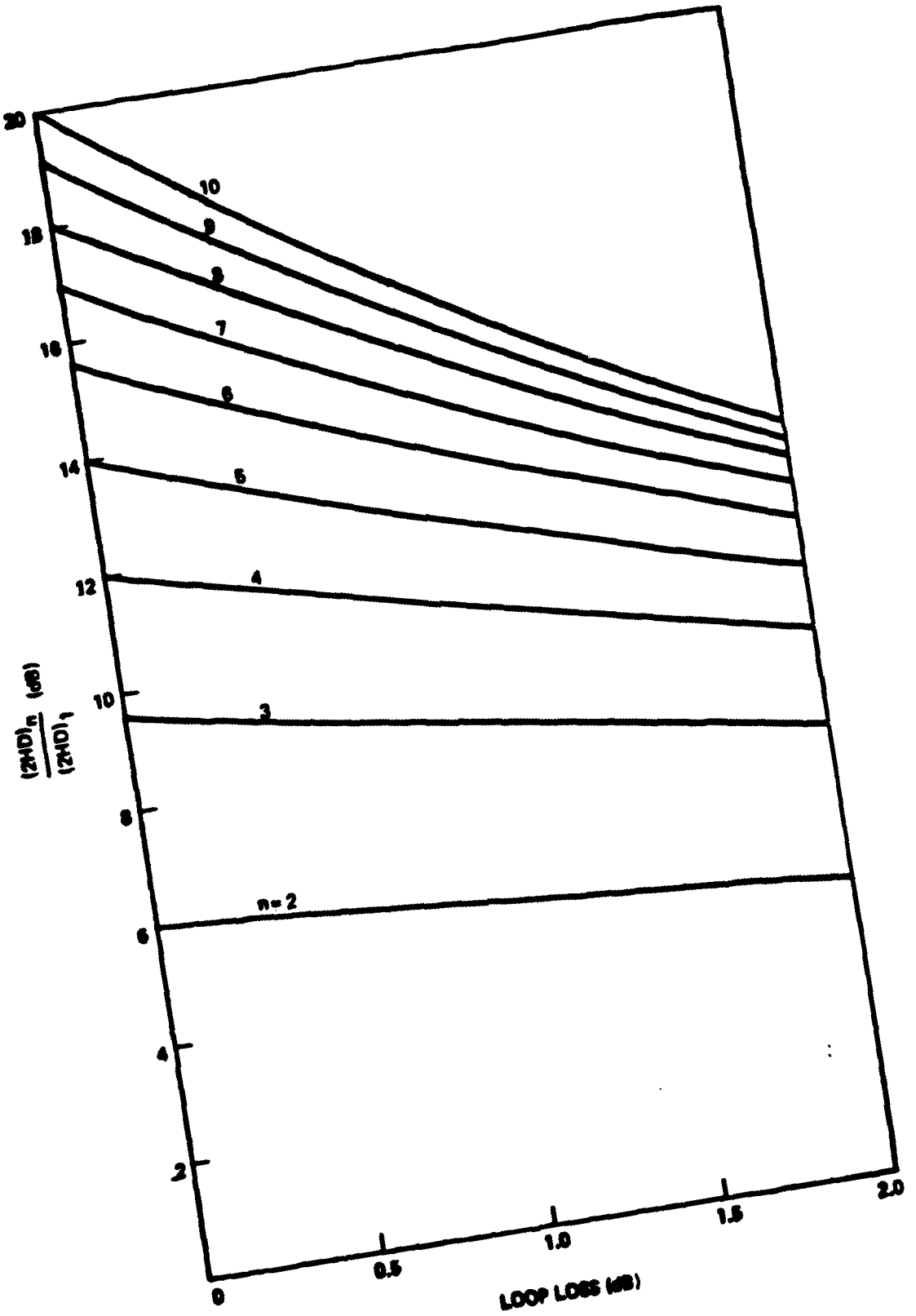

Figure 20. Second harmonic distortion degradation.

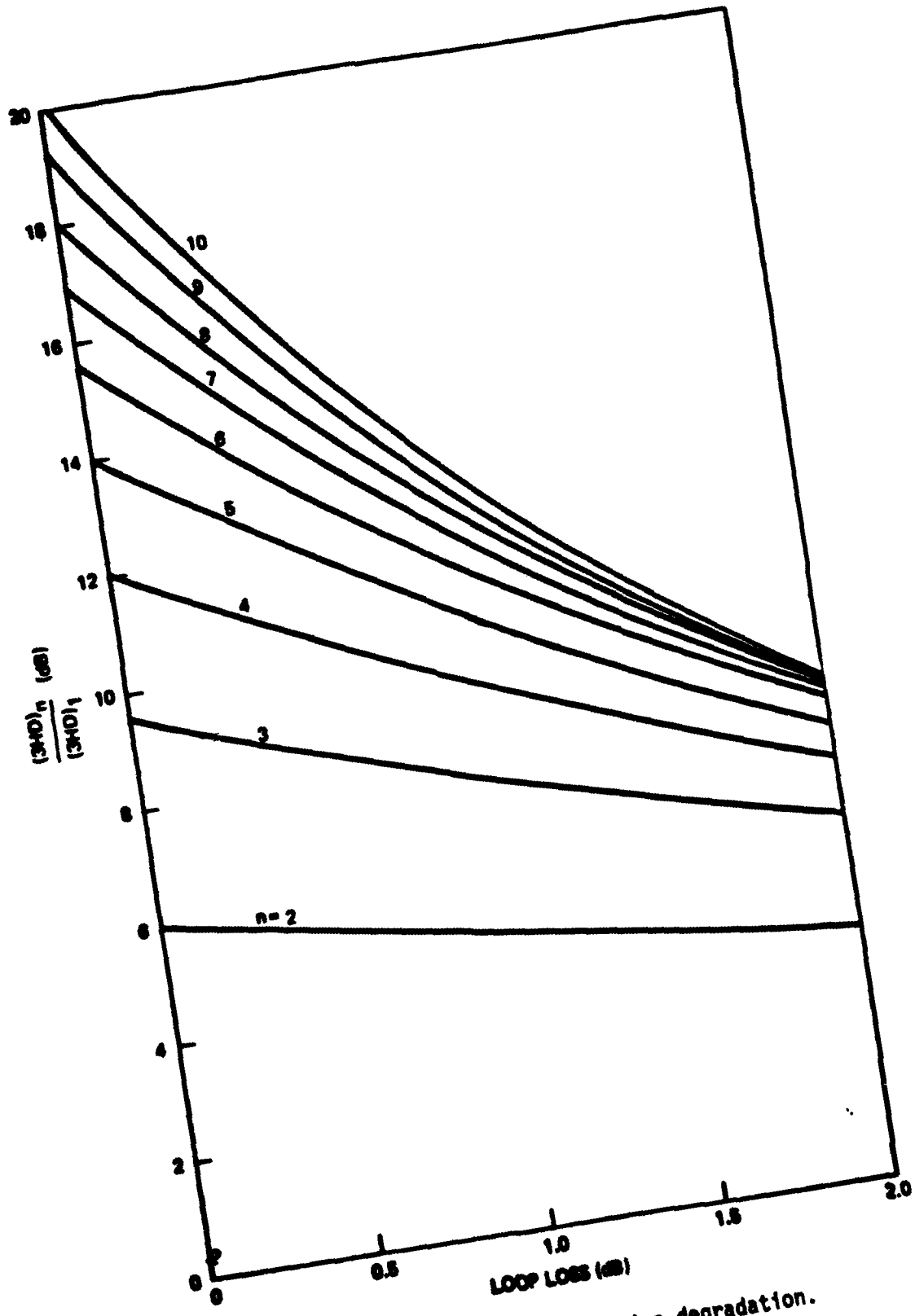

Figure 21. Third harmonic distortion degradation.

2HD <-40 dB	measured relative to the
3HD < -50 dB	fundamental at 500 MHz and 0.5
	modulation index.

where 2HD and 3HD refer to the second and third harmonic distortion.

The distortion is thus dominated by the second harmonic. In addition, second harmonic distortion is normally inversely proportional to the modulation index [3]. Thus, the signal-to-distortion ratio at modulation indices other than 0.5 can be derived from the above specification.

Suppose that we want to achieve a desired value for the final SNR and signal-to-distortion ratio (SDR) at the delay line output. For a given number of circulation n, the initial SNR and SDR requirement after the first circulation can be derived from Figures 19 and 20. Based on the laser nonlinearity properties, the maximum initial modulation index that can still satisfy the initial SNR requirement can then be derived. Then the required input optical power required at the optical receiver input to satisfy the SNR requirement can be evaluated. The maximum allowable fiber length and the achievable delay time can thus be calculated.

A sample result of the above calculation is shown in Figure 22 where the achievable delay time is plotted as a function of the number of circulation n. The parameter values used for the calculation are as follows:

signal-to-noise ratio	SNR = 30 dB
signal-to-distortion ratio	SDR = 30 dB
operating wavelength	λ = 1.3 μm
fiber loss	α = 0.5 dB/km
input equivalent noise resistance of receiver amplifier	R_n = 100 Ω
laser coupled power	P_L = 0 dBm
p-i-n detector quantum efficiency	η = 1 dB
loop loss	β = 1 dB

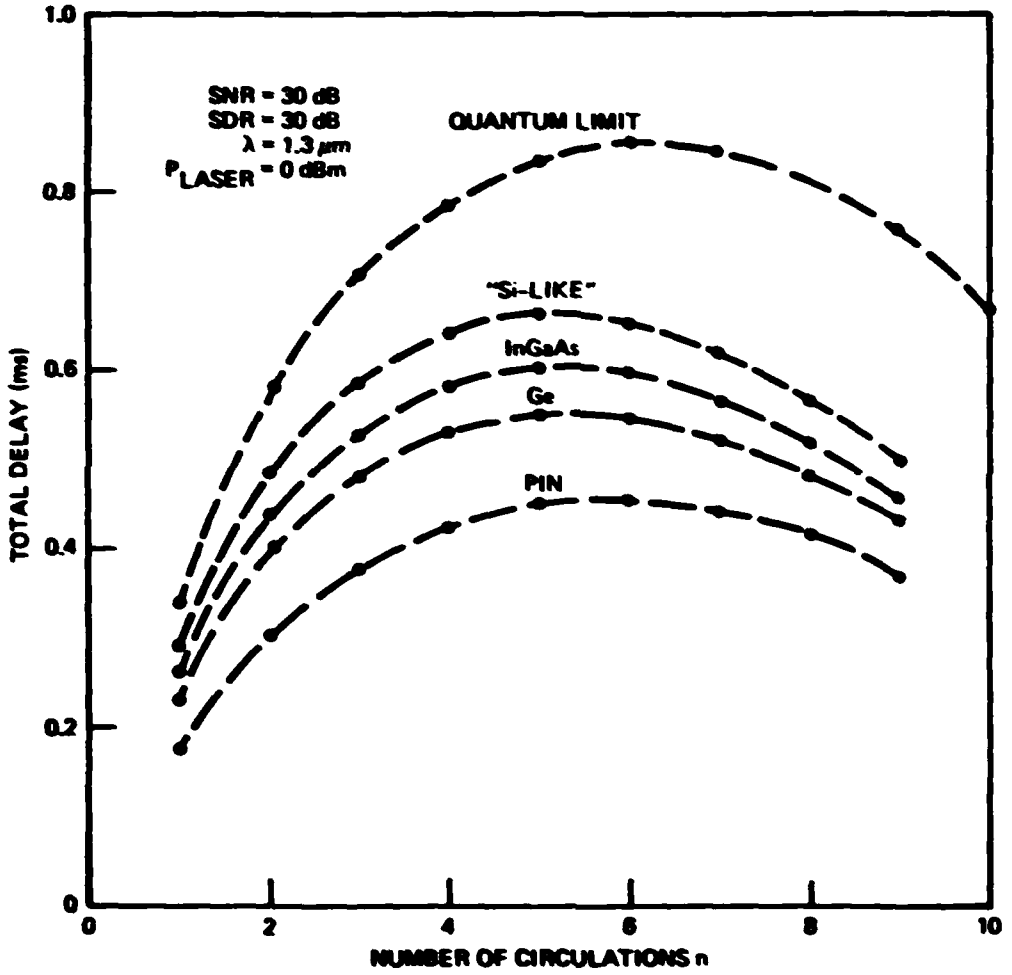

Figure 22. Achievable delay versus number of circulation n for a laser coupled power of 0 dBm and SNR = 30 dB, SDR = 30 dB.

The total achievable delay time is calculated for three representative 1.3 μm photodetectors: an InGaAs p-i-n photodiode, a Ge APD (k=1) and an InGaAs APD (k=0.25). The hypothetical case of a "Si-like" APD (k=0.03) at 1.3 μm and the quantum limit are also included for comparison. It can be observed that there exists an optimum number of circulations that maximize the total delay time. The achievable delay time is 0.46 ms (n=6) for the p-i-n photodiode, 0.55 ms (n=5) for the Ge APD, 0.60 ms (n=5) for the InGaAs APD, 0.66 ms (n=5) for the hypothetical "Si-like" APD, and 0.86 ms (n=6) for the ideal quantum limit case.

It should be noted that the achievable delay times stated above are for the case of a fiber loss of 0.5 dB/km. If fiber loss is lower (e.g. by moving to 1.5 μm region), the delay time is correspondingly higher.

The choice of initial modulation index m_0 to satisfy the requirement of 30 dB final signal-to-distortion ratio at the delay line output is plotted in Figure 23. For the above case, the initial modulation index is 0.4 (for n=5) and 0.35 (for n=6).

The achievable delay time can be increased by improving the laser optical power coupled to the fiber. The achievable delay time has been calculated as a function of the laser coupled power. The results are shown in Figure 24. It can be seen that if the laser coupled power can be improved to 6 dBm, a delay time of approximately 1 ms can be achieved.

The same calculation has been carried out for a delay line SNR and SDR requirement of 25 dB. The choice of initial modulation index to satisfy the 25 dB SDR requirement is shown in Figure 25. The total achievable delay time, as shown in Figure 26. For a laser coupled power of 0 dBm, the achievable delay time is 0.90 ms (n=10) for the p-i-n photodiode, 1.1 ms (n=9) for the Ge APD, 1.21 ms (n=9) for the InGaAs APD, 1.32 ms (n=9) for the hypothetical "Si-like" APD and 1.67 ms (n=10) for the quantum limit case. Thus, for this case, the optimum number of circulation around the loop is 9 or 10, and the initial modulation index is approximately 0.45.

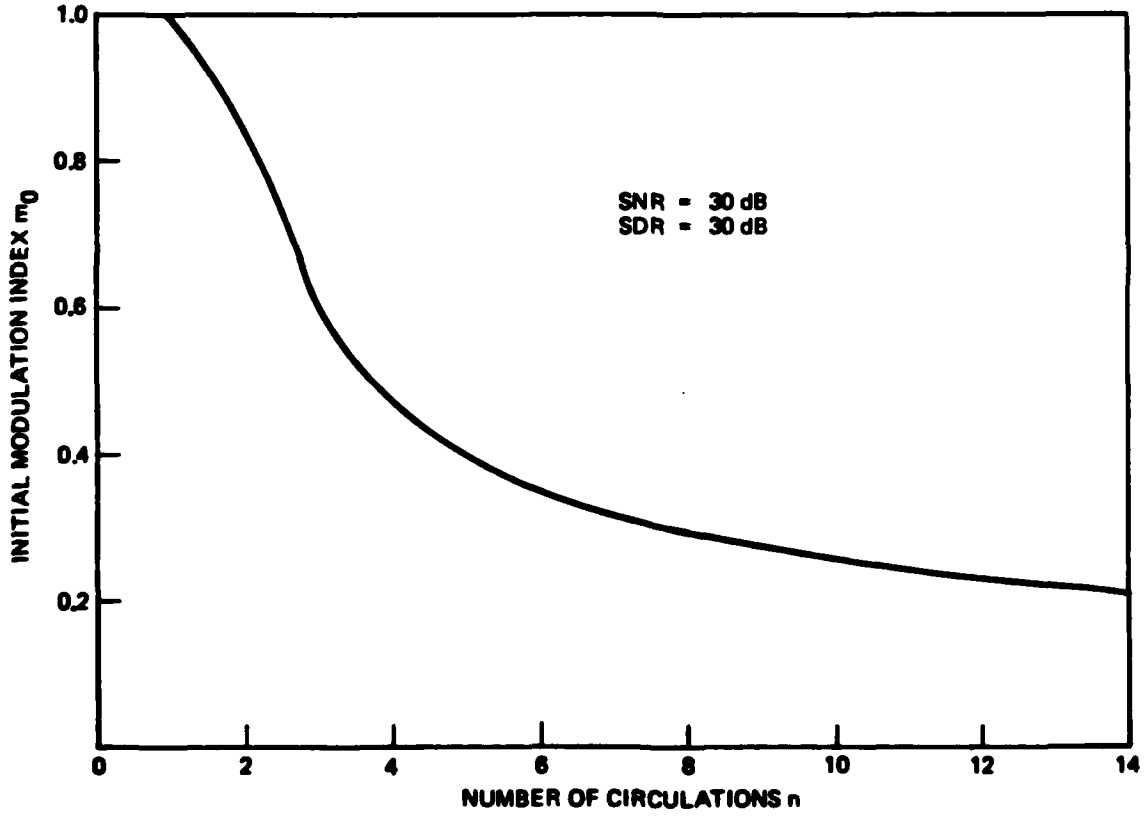

Figure 23. Initial modulation index for SDR = 30 dB.

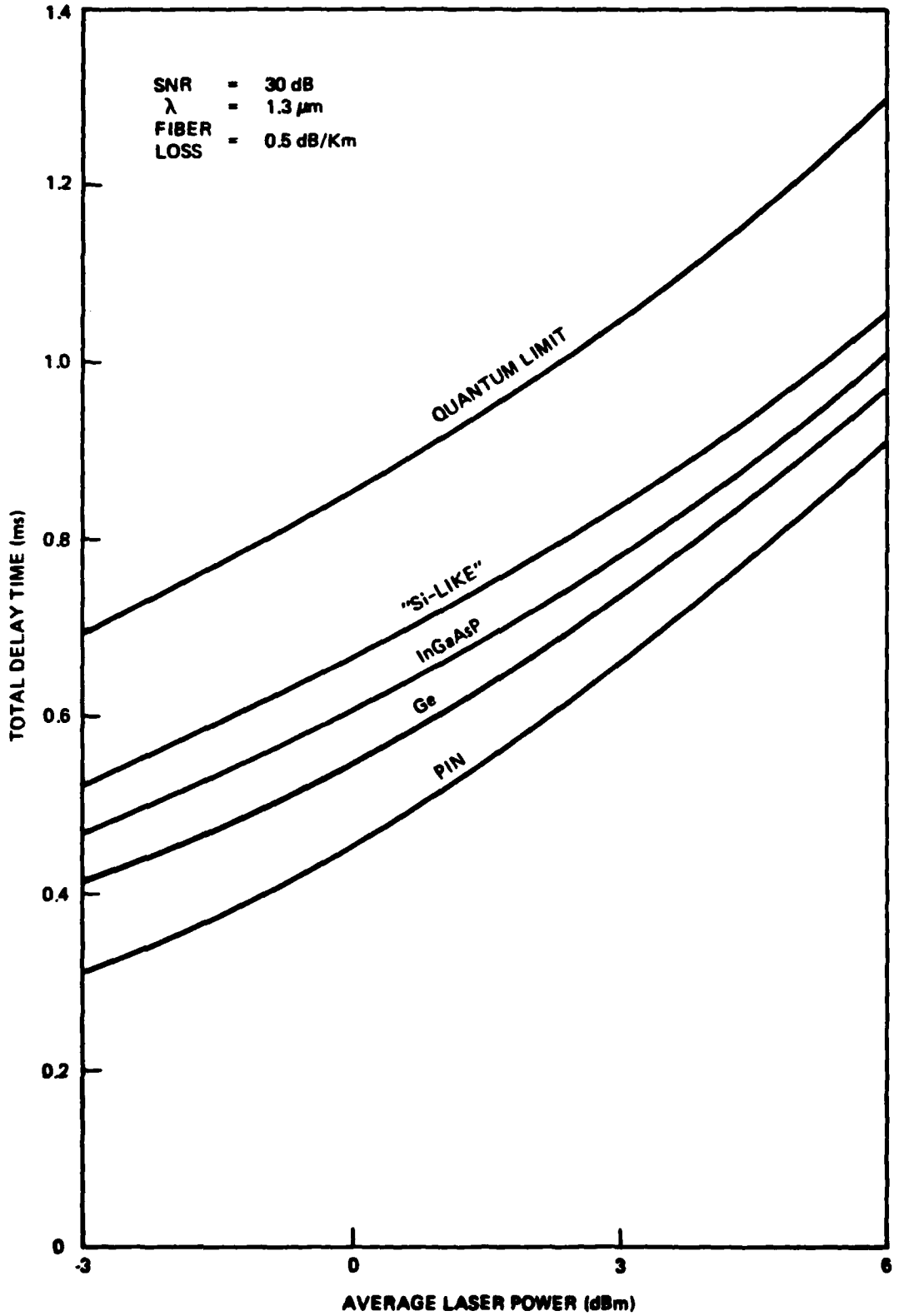

Figure 24. Achievable delay versus laser coupled power for 30 dB SNR & SDR.

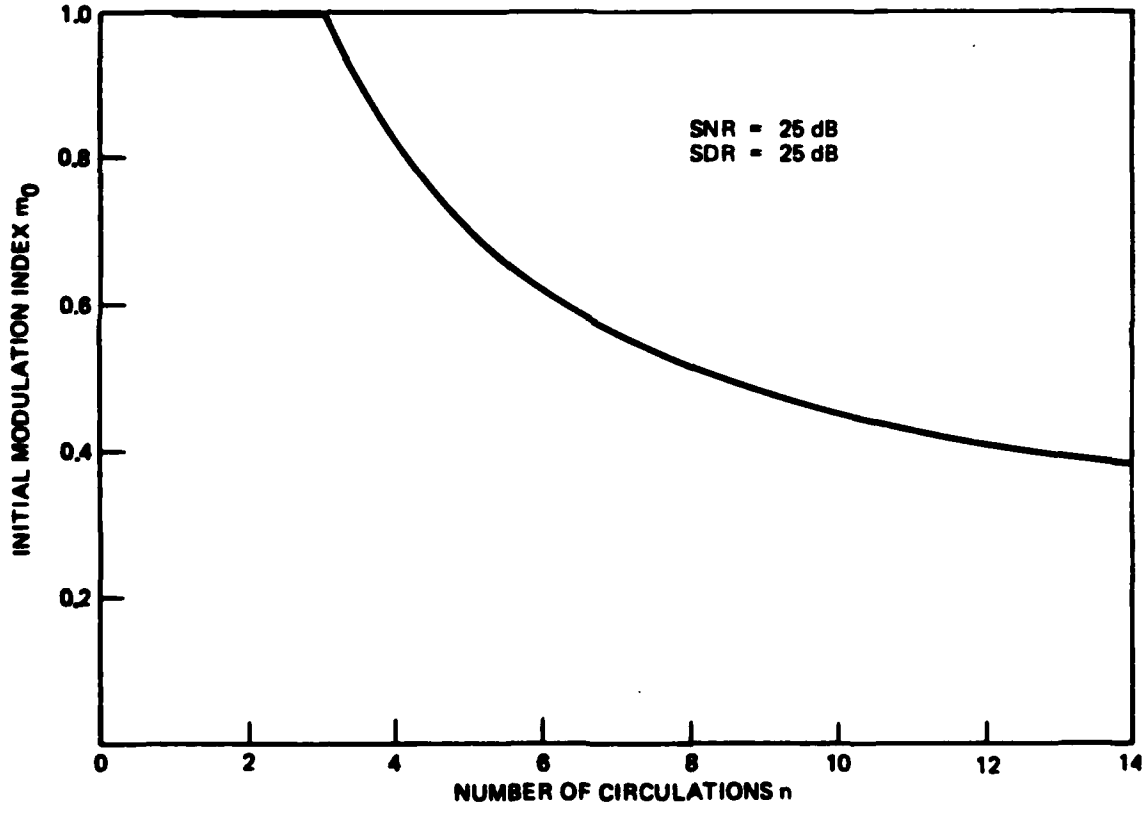

Figure 25. Initial modulation index for SDR = 25 dB.

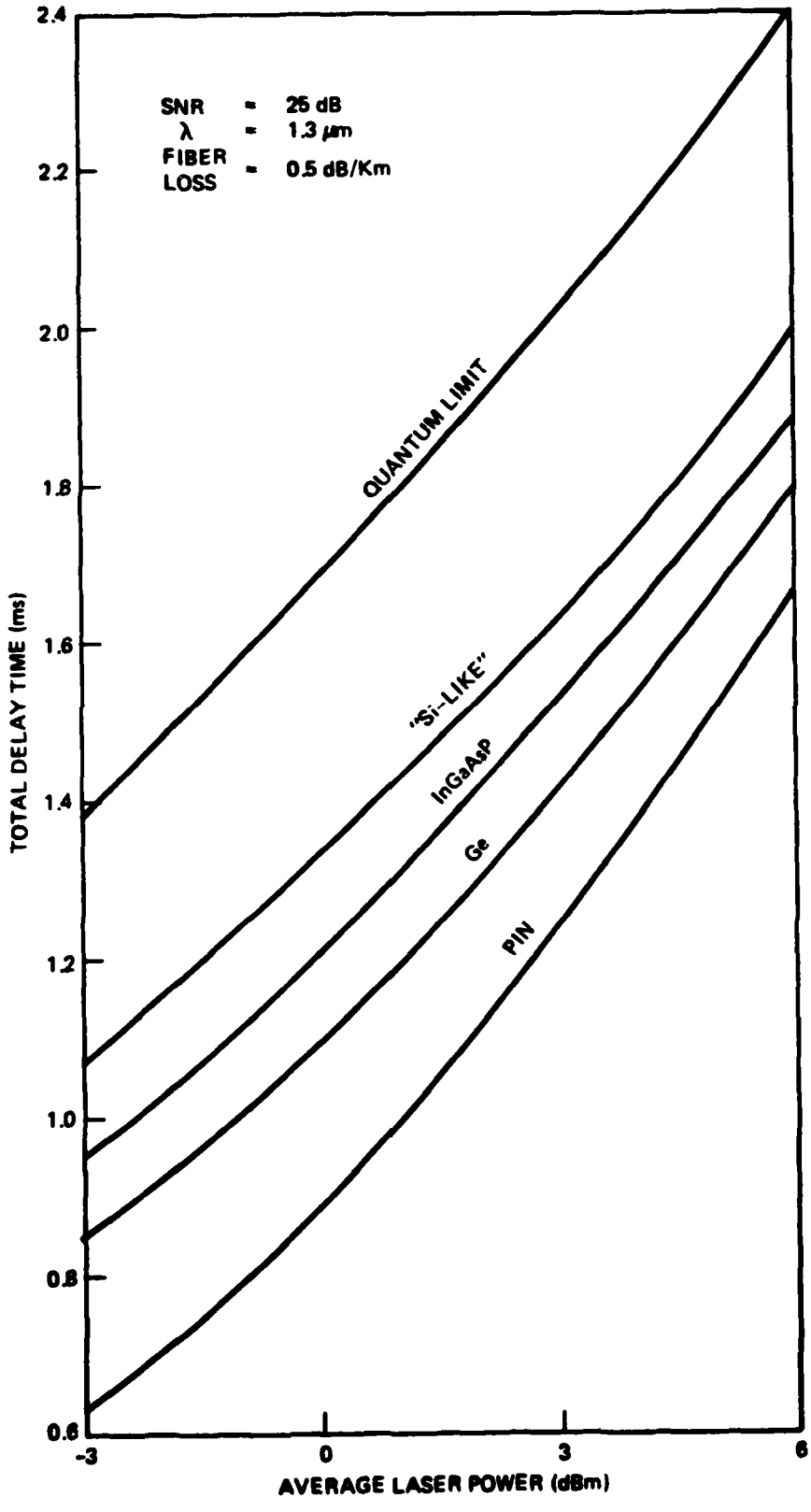

Figure 26. Achievable delay versus laser coupled power for 25 dB SNR & SDR.

3.2 Specifications for a 1 GHz-1ms Delay Line

In this section, we consider the feasibility and necessary component specifications for a delay line with a bandwidth of 1 GHz and a delay time of 1 ms. A simple 1.3 μm p-i-n photodiode is assumed in the optical receiver.

For a total delay time of 1 ms, the total equivalent fiber length (after the optimum number of circulations n) is 200 km. For a delay line bandwidth of 1 GHz, the fiber bandwidth has to be better than 200 GHz-km, preferrably at around 500 GHz-km. In order to achieve this extremely wide bandwidth requirement, the laser wavelength has to be tightly matched to the minimum dispersion length of the fiber. It has been reported that at the minimum dispersion wavelength, a pulse dispersion of less than 30 ps was obtained after transmission through 27 km of single mode fiber. This is equivalent to a fiber bandwidth of more than 200 GHz-km.[4] This wide bandwidth is achieved even when the laser spectral width (FWHM) is 7 nm. For typical laser spectral width of 2 to 4 nm, the 500 GHz-km bandwidth can be achieved readily. In this context, it should be noted that at the minimum dispersion wavelength, the dispersion is proportional to the square of the laser spectral width. Thus a reduction by 2 of the laser spectral width corresponds to a reduction in fiber dispersion by a factor of 4.

The laser wavelength is sensitive to temperature variation. Therefore, in order to maintain the tight matching between the laser wavelength and the fiber minimum dispersion wavelength, the laser has to be temperature-stabilized.

When the above fiber bandwidth condition is satisfied, the pulse dispersion at the final output of the delay line due to fiber dispersion is of the order of 100 ps.

Suppose that a signal-to-noise and signal-to-distortion ratio of 30 dB is required. For a fiber loss of 0.5 dB/km, it can be seen from Figure 24 that in order to achieve 1 ms delay time, a coupled laser power of +7 dBm (5 mW) is necessary. For typical coupling efficiency of 4 dB (40%) from laser to single mode fiber, the laser power into air therefore has to be of the order of 11

dBm (12.5 mW).

The number of circulations in this case is 10. Therefore the initial signal-to-noise ratio requirement can be determined from Figure 19 to be 46 dB. The initial modulation index can be found from Figure 23 to be 0.25 for 10 circulations around the loop. The above requirements translate to a dc-signal-to-noise ratio of 148 dB/Hz for the laser. This is indeed a very tight requirement considering the fact that this is the laser noise after the effects of optical feedback, mode partition noise and modal polarization noise.

The above design process can be repeated for the case of 25 dB SNR and SNR. From Figure 26, a coupled laser power of 1 dBm (1.25 mW) is required. The number of circulations in this case is also 10. Thus the initial modulation index can be found from Figure 25 to be 0.45. The initial signal-to-noise ratio requirement can be determined from Figure 19 to be 41 dB. Therefore, the required dc-signal-to-noise ratio of the laser is 138 dB/Hz.

3.3 1.55 μm Wavelength Operation

The previous cases are for an operating wavelength at the minimum dispersion wavelength around 1.3 μm . In this section, we consider the delay line operating at the minimum loss wavelength of silica fibers which is around 1.55 μm .

There are two alternatives of operating at 1.55 μm in order to avoid the fiber dispersion problem. One approach is to use standard single mode fiber with minimum disperson at 1.3 μm . For operation at 1.55 μm , these fibers typically have a dispersion coefficient of 15 to 20 ps/km/nm. Thus, a truly single longitudinal mode laser, (even under direct modulation) is required to avoid the fiber dispersion. This laser is often referred to as single mode stabilized laser or dynamic single mode (DSM) laser. Mode stabilization is necessary because nominally single mode lasers at CW tend to oscillate in many modes when being directly modulated. Dynamic single mode lasers have been achieved by a variety of techniques: distributed feedback (DFB)[5],

distributed Brag reflector (DBR)[6], injection locking[7], external cavity[8], short cavity[9], two-cavity (or two-section)[10], short-coupled-cavity (SCC)[11], and cleaved-coupled-cavity (CCC or C^3)[12]. The line widths of these stabilized lasers are in the order of 1A. Thus even with the large fiber dispersion coefficient, the pulse dispersion at the fiber output is negligible.

The second approach for 1.55 μm operation is to design the fiber such that the minimum dispersion wavelength coincides with minimum loss wavelength at around 1.55 μm . Consequently, a standard nominally single mode laser can be used. The fiber minimum dispersion wavelength can be shifted to 1.55 μm by decreasing the fiber core diameter and increasing the refractive index difference between the core and cladding (e.g. by using higher dopant concentration). These fibers are often referred to as dispersion-shifted fiber. However, the loss of dispersion-shifted fibers tend to be higher than standard fibers. The best reported value for dispersion-shifted fiber loss at 1.55 μm is 0.24 dB/km[13], as compared to 0.2 dB/km[14] for standard fibers.

Out of these two approaches, the first approach of using standard fibers with minimum dispersion at 1.3 μm and dynamic single mode lasers is more advantageous. The fiber loss at 1.55 μm is lower and splice and connector losses can be expected to be lower because of the larger core size. The laser is truly single mode with its oscillating wavelength stabilized. Thus problems associated with mode partition noise, mode hopping due to spectral instability are minimized if not eliminated. Furthermore, matching of the fiber minimum dispersion wavelength and the laser wavelength is not required. Dynamic single mode lasers are under intensive research and development because of the interest in long hand high capacity transmission for telecommunications application. Thus, considerable improvement in their characteristics can be expected.

For the delay line performance evaluation, we assume a fiber loss (including splices) of 0.25 dB/km. This value is applicable for both of the above approaches. Since this is half the loss value assumed at 1.3 μm , considerable improvement can be expected. The achievable delay times are twice the values given in Figures 24 and 26.

First, let us consider the case of 30 dB SNR and SDR. For 1 ns delay time, the laser output coupled is determined from Figure 24 to be about 1 dBm (1.25 mW). The number of circulations in this case is 6. Thus the initial signal-to-noise ratio requirement is found from Figure 19 to be 44 dB. The initial modulation index is given from Figure 23 as 0.35. Thus the required dc signal-to-noise ratio of the laser is 143 dB/Hz.

For the case of 25 dB SNR and SDR, the laser coupled power requirement can be determined from Figure 26 to be about -6 dBm. The required number of circulations is also 6. The initial signal-to-noise ratio is given from Figure 19 as 39 dB. The initial modulation index is given from Figure 25 as 0.6. Therefore the required dc signal-to-noise ratio requirement for the laser is 134 dB/Hz.

A summary of the laser and fiber specifications for a 1 GHz-1 ms delay line is shown in Table 1. We can observe that with present state-of-the-art devices and fibers, a SNR and SDR of 25 dB can be readily achieved at 1.3 μm operating wavelength. The main problem here is tight matching between the laser wavelength and the fiber minimum dispersion wavelength. By shifting to the longer operating wvelength of 1.55 μm , a SNR and SDR of 30 dB can be obtained with present devices and fibers. This can be achieved by either of the two approaches outlined earlier (using standard fibers and dispersion-shifted fibers). The first approach of using standard fibers and dynamic single mode lasers is much more advantageous.

3.4 Proposed Delay Line for Immediate Implementation

In this section, we consider a recirculating delay line that can be implemented with commercially available components at present.

For the laser diode, we can take the optical power coupled to the single mode fiber pigtail to be -3 dBm (0.5 mW). This value is readily achieved with present components such as the BH laser (HLP-5000-S) from Hitachi. The dc signal-to-noise ratio is assumed to be better than 140 dB/Hz. The second harmonic distortion is taken to be 40 dB below the fundamental at a modulation index of 0.5.

OPERATING WAVELENGTH		1.3 μm		1.5 μm	
Required SNR & SDR		30 dB	25 dB	30 dB	25 dB
LASER	dc SNR (dB/Hz)	148	138	143	134
	2HD (dB)	40	50	40	40
	3HD (dB)	50	50	50	50
	Coupled Power (dBm)	7	1	1	-6
	Flat Bandwidth (GHz)	1	1	1	1
FIBER	Bandwidth (GHz-km)	500	500	500	500
	Loss (dB/km) (including splices)	0.5	0.5	0.25	0.25
	Length required (km)	20	20	33	33

Table 1. Required specifications of lasers and fibers for a 1 GHz-1ms delay line.

For the fiber, we assume a standard single mode fiber with a minimum dispersion wavelength at 1.3 μm and a loss of 0.5 dB/km (including splices) at 1.3 μm .

The SNR and SDR of the delay line output is taken to be 25 dB. It can be seen from Figure 26 that a total delay time of 0.63 ms can be achieved. The number of circulations in this case is n=8 and the initial modulation idex is m=0.5. The fiber length required is thus calculated to be 16 km. The initial SNR after the first circulation can be derived from Figure 19 to be 38 dB. The required dc signal-to-noise ratio of the laser is therefore 134 dB/Hz which is well within the assumed value of 140 dB/Hz.

In summary, the proposed system would have the laser operatiang at an average coupled output power of -3 dBm and an initial modulatin index of 0.5. The fiber length used is 16 km, corresponding to a total fiber loss (in one circulation) of 8 dB. The output power incident on the optical receiver is thus -11 dBm. After the first circulation, the SNR at the optical receiver output is 38 dB and the SDR is 40 dB. As the signal recirculates through the loop, the SNR and SDR are reduced. Finally, after 8 recirculations corresponding to a total delay time of 0.63 ms, the SNR and SDR obtained is 25 dB.

4. LASER TRANSMITTER

As discussed in the previous section, the performance of the laser transmitter is very critical to the delay line operation. The laser has to satisfy the specified requirements with regard to its coupled power, noise, spectrum characteristics, harmonic distortion, bandwidth... Coupling method between the laser and the single mode fiber is also important because of potential noise and distortion enhancement due to optical feedback to the laser cavity. Therefore, the selection of the laser and its package is very critical. Since mode-stabilized dynamic single mode lasers are not commercially available at present, we have to select the laser from a variety of nominal single mode lasers. These typically have index-guided structures such as BH, CSP, TJS... Also for operation at 1.3 μm , the laser wavelength has to be selected to match the fiber minimum dispersion fiber.

It has been determined previously that for 1.3 μm operation, a laser coupled power of 7 dBm is necessary for 30 dB SNR and SDR. The development of high power lasers at 1.3 μm is thus very beneficial. We have undertaken an investigation of the possible output power and limitation of high power lasers. The results are given in Appendix 1.

In addition to the laser optical power and noise characteristics, the laser transmitter itself has to satisfy the electrical characteristics regarding impedance matching and transfer function. A input VSWR of less than 2:1 is desirable over the 0-1 GHz frequency band. The frequency response of the laser transmitter should be flat to ±0.25 dB over the above working frequency band.

To determine the feasibility of such a flat bandwidth laser transmitter, we have designed and fabricated a breadboard transmitter. The laser used is a Hitachi buried heterostructure laser at 1.3 μm (HLP 5500) in a fiber pigtail package which is mounted on a 50 ohm micro strip line configuration. The laser stray and package capacitance and inductance are taken into account in designing the microstrip circuit. A photograph of the breadboard transmitter is shown in Figure 27. Its frequency response is measured by using the ultrafast p-i-n detector (QD-100-UHS from Lasertron). The frequency response

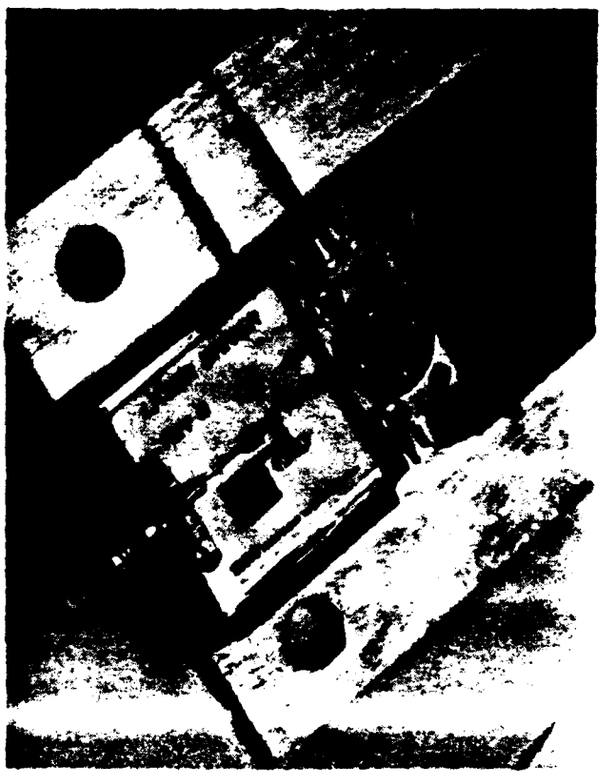

Figure 27. 1.3 μm laser transmitter breadboard.

measured on the 1.3 GHz optical network analyzer is shown in Figure 28. It can be observed that the response is flat to ±0.25 dB over the 0-1.3 GHz frequency band of the test instrument. Another measurement up to 2.5 GHz using the sweep frequency synthesizer and spectrum analyzer arrangement is shown in Figure 29. The response is flat to ±0.5 dB up to 2.5 GHz.

The above excellent performance was achieved even when the laser is already packaged. In the next phase of the program, the laser will probably be purchased in chip form on a submount to eliminate extra stray capacitance and inductance due to the package. Thus even better performance can be expected.

A passive laser driver as described previously has the advantage of simplicity and excellent linearity. An obvious disadvantage is that since the laser transmitter input impedance is 50 ohm, the driving voltage swing can be quite high. However, if BH lasers with a threshold current of 15 mA are used, the driving voltage swing required is only 750 mV for a modulation up to twice the threshold. This level can be readily accomodated by the interface amplifier.

An active laser transmitter using either GaAs MESFET's or silicon microwave bipolar transistor can also be used. However, it is more complex and linearity in an issue. Therefore, it was decided that a passive laser driver as described previously is a better choice.

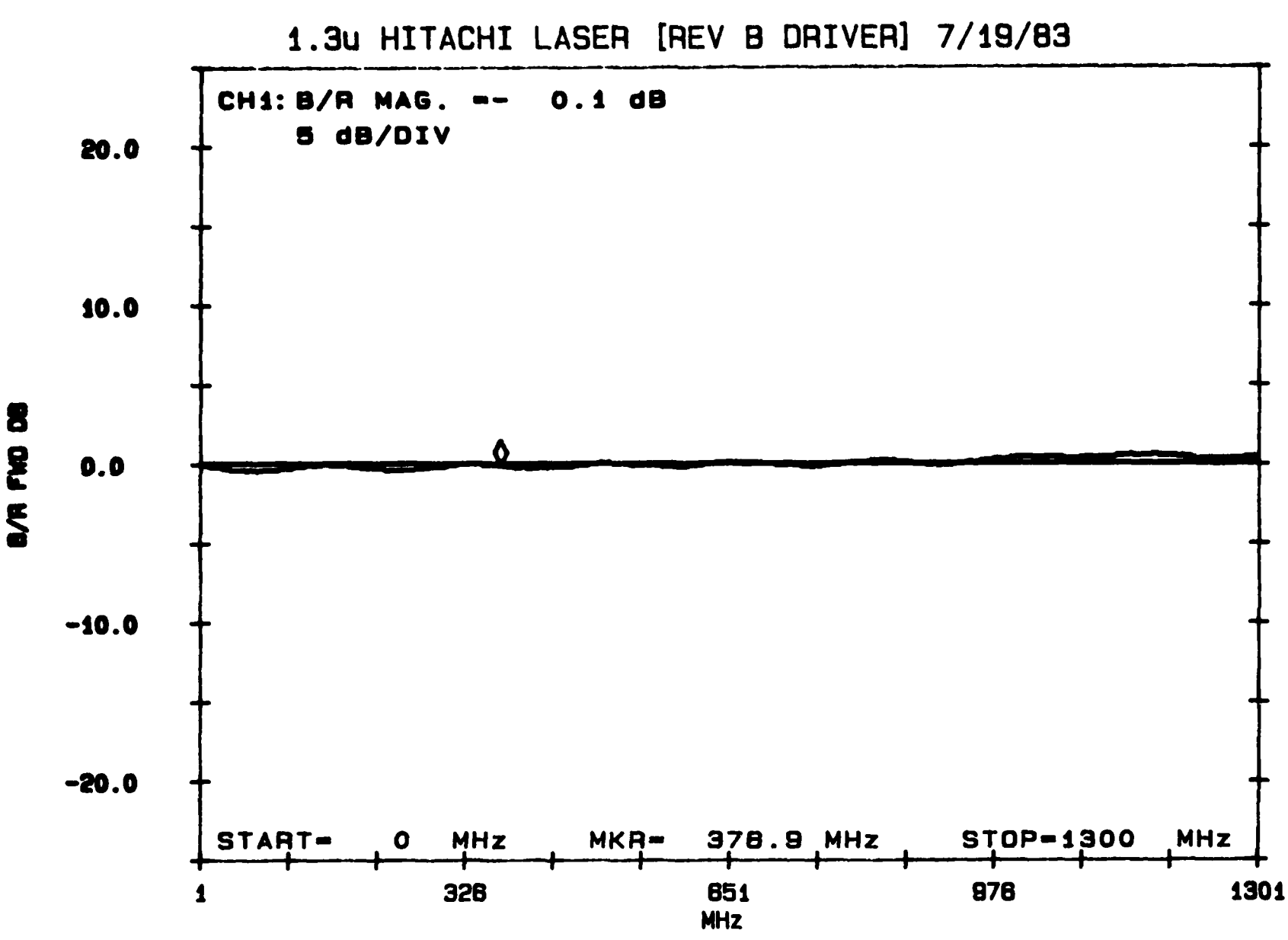

Figure 28. Frequency response of laser transmitter.

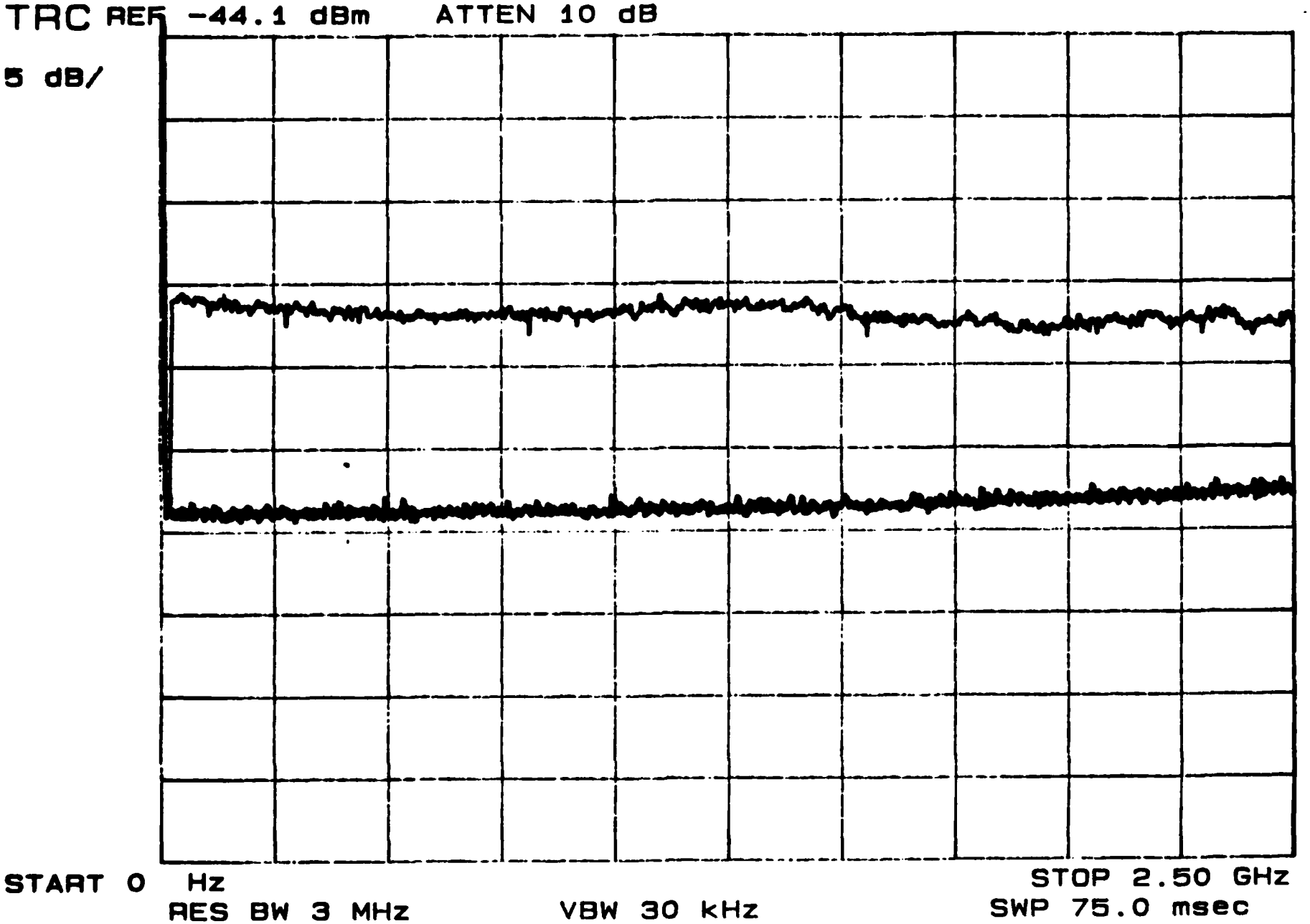

Figure 29. Frequency response of laser transmitter up to 2.5 GHz.

5. CONCLUSIONS

In this report, we have investigated the feasibility of realizing a 1 GHz-1ms recirculating delay line using single mode fibers as the delay medium. The total achievable delay time was predicted for various types of photodetectors as well as signal-to-noise ratio and signal-to-distortion ratio requirement. It was shown that with present state-of-the-art components, a SNR and SDR of 25 dB can be readily achieved at 1.3 μm operating wavelength. By shifting to 1.55 μm wavelength, a SNR and SDR of 30 dB can be obtained. This can be achieved by two approaches: (1) using standard fiber with minimum dispersion at 1.3 μm and dynamic single mode lasers or (2) using dispersion-shifted fiber with minimum dispersion at 1.55 μm and nominally "single mode" lasers. The first approach is more advantageous because of minimum noise due to laser-fiber interactions (mode partition, optical feedback, ...) and there is no need for tight matching of the laser wavelength and fiber minimum dispersion wavelength. On the other hand, if for some other reason operation at 1.3 μm wavelength is required, then a higher power "single mode" laser with 7 dBm coupled optical power output needs to be developed in order to satisfy the 30 dB SNR and SDR requirement. We have also indicated other required specifications for the laser and fiber in each of the above cases.

Several key components that are essential towards the realization of the delay line have also been demonstrated. An optical receiver with a ±0.25 dB flat bandwidth of more than 1.3 GHz has been fabricated. In fact the receiver response is ±0.5 dB flat to 2 GHz. The receiver also has an extremely low noise level. The input equivalent noise spectral density is measured to be $9pA/\sqrt{Hz}$ with a noise corner frequency of 920 MHz. This corresponds to an input equivalent noise resistance of 146 ohm over the 0-1 GHz frequency band.

A laser transmitter breadboard has also been fabricated and tested. A frequency response of ±-.25 dB flatness up to 1.3 GHz was also demonstrated. The laser transmitter is ±0.5 dB flat up to 2.5 GHz.

In summary, the feasibility of the optical components have already been demonstrated. The remainder of the system is fully electronic and can be

readily implemented using microwave circuit techniques. Therefore, with the proper choice of laser and fiber, a delay line of 1 GHz bandwidth and 1 ms delay time can be realized.

REFERENCES

1. T.V. Muoi, "Receiver Design for High Speed Optical Fiber Systems", submitted to IEEE Jour. Lightwave Technology.

2. R.G. Smith and S.D. Personick, "Receiver Design for Optical Fiber Communication Systems", Chapter 4 in Semiconductor Devices for Optical Communication, Springer-Verlat, New York, 1980.

3. K. Stub Kjaer and M. Danielsen, "Nonlinearities of GaAlAs Lasers-Harmonic Distortion", IEEE Jour. Quant. Elect. Vol. QE-16, pp. 531-537, May 1980.

4. C. Lin et al, "Picesecond Dispersionless Transmission of InGaAsP Injection Laser Pulses at the Minimum Chromatic Dispersion Wavelength in a 27 km Long Single Mode Fibre", Elec. Lett., Vol. 18, pp. 882-884, Sept. 1982.

5. S. Akiba et al, "Distributed Feedback InGaAsP/InP Lasers With Window Region Emitting at 1.5 μm Range", IEEE Jour. Ouant. Elect., Vol. QE-14, pp. 1052-1056, June 1983.

6. F. Koyama et al, "1.5 - 1.6 μm GaInAsP/InP Dynamic Single Mode Lasers with Distributed Bragg Reflector", IEEE Jour. Quant. Elec., Vol. QE-19, pp. 1042-1051, June 1983.

7. S. Kobayashi et al, "Single Mode Operation of 500 Mbits/s Modulated AlGaAs Semiconductor Laser by Injection Locking", Elec. Lett., Vol. 16, pp. 746-748, Sept. 1980.

8. K.R. Preston et al, "External Cavity Controlled Single Longitudinal Mode Laser Transmitter Module", Elec. Lett., Vol. 17, pp. 931-933, Nov. 1981.

9. T.P. Lee et al, "Short-Cavity Single Frequency InGaAsP Buried Heterostructure Lasers", Elec. Lett., Vol. 19, pp. 82-84, Feb. 1983.

10. K.J. Ebeling et al, "Generation of Single Longitudinal Mode Subnanosecond Light Pulses by High Speed Current Modulation of Monolithic Two-Section Semiconductor Lasers", Elec. Lett., Vol. 18, pp. 901-902, Oct. 1982.

11. C. Lin et al, "Short-Coupled-Cavity (SCC) InGaAsP Injection Lasers for CW and High Speed Single Longitudinal Mode Operation", Elect. Lett., Vol. 19, pp. 561-562, July 1983.

12. W.T. Tsand et al, "Stable Single Longitudinal Mode Operation Under High Speed Direct Modulation in Cleaved-Coupled-Cavity GaInAsP Semiconductor Lasers", Elect. Lett., Vol. 19, pp. 488-490, June 1983.

13. B.J. Ainslie et al, "Monomode Fiber With Ultralow Loss and Minimum Dispersion at 1.55 μm ", Elec. Lett., Vol. 18, pp. 842-844, Sept. 1982.

14. T. Miya et al, "Ultimate Low Loss Single Mode Fiber at 1.55 μm ", Elec. Lett., Vol. 15, pp. 106-108, 1979.

Figure Captions

APPENDIX 1

HIGH POWER LONG WAVELENGTH LASERS

1.1 Introduction

Factors limiting maximum power levels of semiconductor lasers include heat sinking, facet damage, mode stability and degradation. While heat sinking and degradation influence the long term reliability, facet damage and mode stability must be considered for short term operation.

1.2 Device Considerations

1.2.1 Catastrophic Mirror Damage

Catastrophic mirror damage (CMD) can limit the maximum power delivered by a semiconductor laser. This is caused by heating due to absorption of optical power at the mirror facet where a high density of surface recombination centers reside. Above a critical optical power density, the active layer melts and CMD results. For GaAs/AlGaAs lasers, CMD occurs at approximately 15 $mW/\mu m^2$ [Ref. A1] for CW operation. Long wavelength devices based on the InGaAsP/InP material system have shown higher damage thresholds of $\gtrsim 45$ $mW/\mu m^2$. Higher powers can be sustained by facet coating. This is regularly applied to many GaAs/AlGaAs lasers to increase the maximum power and device reliability, but has not been considered to be essential for InGaAsP lasers.

1.2.2 Mode Stability

Although not a limit to high power operation, mode stability is important in applications where coupling, focusing or linearity are critical. Often, stable operation in the fundamental transverse is preferred. This can be achieved by a suitably chosen waveguide structure for the laser. For example, the buried heterostructure (BH) laser [Ref. A2] (Figure A1), which has a rectangular slab waveguide, can be fabricated so as to eliminate the higher order mode. For a 0.1 μm thick active layer, this cutoff occurs when the waveguide width is less than 2 μm.

A single longitudinal mode is sometimes also desirable, such as in single mode high bandwidth communication links. While some commercial laser claim single longitudinal mode, they do not possess any mechanism that effectively eliminates other modes. Even if a single mode exists under d.c. bias, other modes usually appear at high modulation rates. Noteworthy among various

"active" mechansims devised for single mode operation are: (A) short cavity ($< 100\ \mu$ compared to $300\ \mu$)[3] [Ref. A3]; (B) 3-mirror cavity[Ref. A4]; and (C) cleave coupled cavity[Ref. A5]. Method (A) widens the cavity Fabry-Perot mode separation so that only one mode lies close to the gain peak. However, the short cavity also reduces the output power drastically. (B) and (C) uses interference between two F-P cavities also to separate the resonating modes further. Method (C) has also been demonstrated to possess tuning capability.

1.2.3 Heat Sinking

Since laser threshold I_{th} increase with temperature by $I_{th} \alpha \exp(T/T_o)$, where T_o is typically 60-80°K, thermal runaway may occur when the device is operated CW with a poor heat sink. Presently heat sink thermal resistances of $\sim$ 15-20° C/W can be routinely produced. These values are adequate for most lasers with operating currents $<$200 mA. For optimum heat dissipation, the laser active area should also be increased.

1.2.4 Long Term Reliability

This is one area where less quantitative statistical data is available. The general fact is shorter lifetime at higher temperatures and higher optical power densities. Expected lifetimes at 6 mW, 25°C is in excess of 10^4 hours. Therefore, for initial short term studies, this is not expected to pose any serious problem.

1.3 High Power Laser Designs

In light of the above discussions, a high power 1.3 μ laser ($\gtrsim$10 mW) can easily be fabricated even without facet coating. A buried heterostructure laser with 2 μ wide active region can be biased way above threshold to output such power. However, for reliability consideration, this may not be desirable. Other methods that have been suggested include various ways to increase the lasing spot size to lwer the optical power density both at the mirror and in the waveguide. This also facilitates heat dissipation from the active region. For example, by using a strip loaded structure[Ref. A6], the lasing spot size can be widened to 5 μ while still maintaining single lateral mode. With this structure, power as high as 40 mW can be achieved. Another method, aimed at attaining very high power, combines laser outputs from several lasers coherently. These phase locked arrays have produced output powers as high as 1.5 W CW in GaAs/AlGaAs[Ref. A7] lasers. The same concept can be applied to quaternary InGaAsP lasers.

1.4 Suggested Laser Designs

1.4.1 High Power Strip Loaded Lasers

The design is shown in Figure A2. The active layer is "strip loaded" by lightly etching the sides either by wet chemical or dry etching. A regrowth of semi-insulating InP on the sides will provide perfect current confinement and ensure low threshold current. We expect I_{th} ~40-60 mA and power output easily in excess of 30 mW. The growth of semi-insulating InP has recently been demonstrated in our laboratory. In our opinion, this structure is the simplest way to achieve powers up to 30 mW.

The only drawback is the unknown reliability of such a laser. Regrowth is routinely performed in BH laser fabrication and does not seem to affect reliability adversely. However, the dopants used in obtaining the S.I. InP could contribute to degradation, although the doping level is so low that we do not think it would.

1.4.2 Curved Waveguide Structure

As illustrated in Figure A3, the active layer is curved as a result of growth on an etched channel. This structure has been demonstrated by Murotani[Ref. 8A] et.al. and in excess of 6 mW at $2I_{th}$. With further improvement in growth control, 10 mW should be possible.

1.5 Conclusion

In conclusion, it is our view that output powers of 30 mW or more can easily be within reach of our present technology.

References for Appendix

A1. T. Kamejima and H. Yonezu, "Catastrophic Optical Damage Generation Mechanism in (AlGa)As DH Lasers", Japan. J. Appl. Phys. supplement 19-1, pp. 425-429 (1978).

A2. M. Hirao, A. Doi, S. Tsuji, M. Nakamura, and K. Aiki, "Fabrication and Characterization of Narrow Stripe InGaAsP/InP Buried Heterostructure Lasers", J. Appl. Phys. 51, 4539, (1980).

A3. C.A. Burrus, T.P. Lee, and A.G. Dentai, "Short-Cavity Single-Mode 1.3 μm InGaAsP Lasers with Evaporated High-Reflectivity Mirrors", Electron. Lett., 17, pp. 954-956, (1981).

A4. Hong K. Choi and Shyh Wange, "Semiconductor Internal-Reflection-Interference Laser", Appl. Phys. Lett., 40, pp. 571-573, (1982).

A5. W.T. Tsang, N.A. Olsson, and R.A. Logan, "High-Speed Direct Single-Frequency Modulation with Large Tuning Rate and Frequency Excursion in Cleave-Coupled-Cavity Semiconductor Lasers", Appl. Phys. Lett., 42, pp. 650-652, (1983).

A6. W.T. Tsang and R.A. Logan, "GaAs-$Al_xGa_{1-x}As$ Strip Buried Heterostructure Lasers", J. Quan. Electron., QE-15, pp. 451-469, (1979).

A7. D.R. Scifres, R.D. Burnham, C. Lindstrom, W. Streifer, and T.L. Paoli, "Phase-Locked (GaAl)As Laser Emitting 1.5 W CW per Mirrow", Appl. Phys. Lett., 42. ½½/ 645-647, (1983).

A8. T. Murotani, E. Oomura, H. Higuchi, H. Nakamura, W. Susaki, "InGaAsP/InP Buried Crescent Laser Emitting 1.3 μm with Very Low Threshold Current", Electron. Lett., 16, pp. 566-568, (1980).

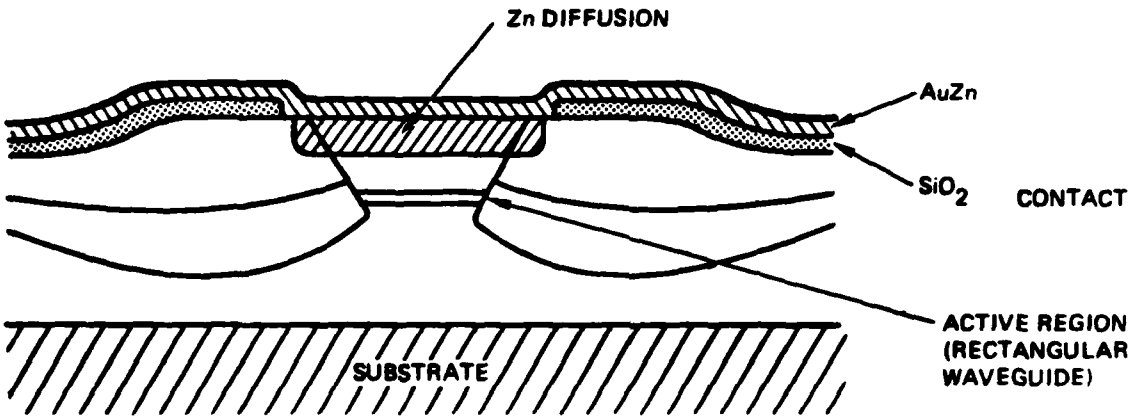

Figure A1. Buried Heterostructure Laser.

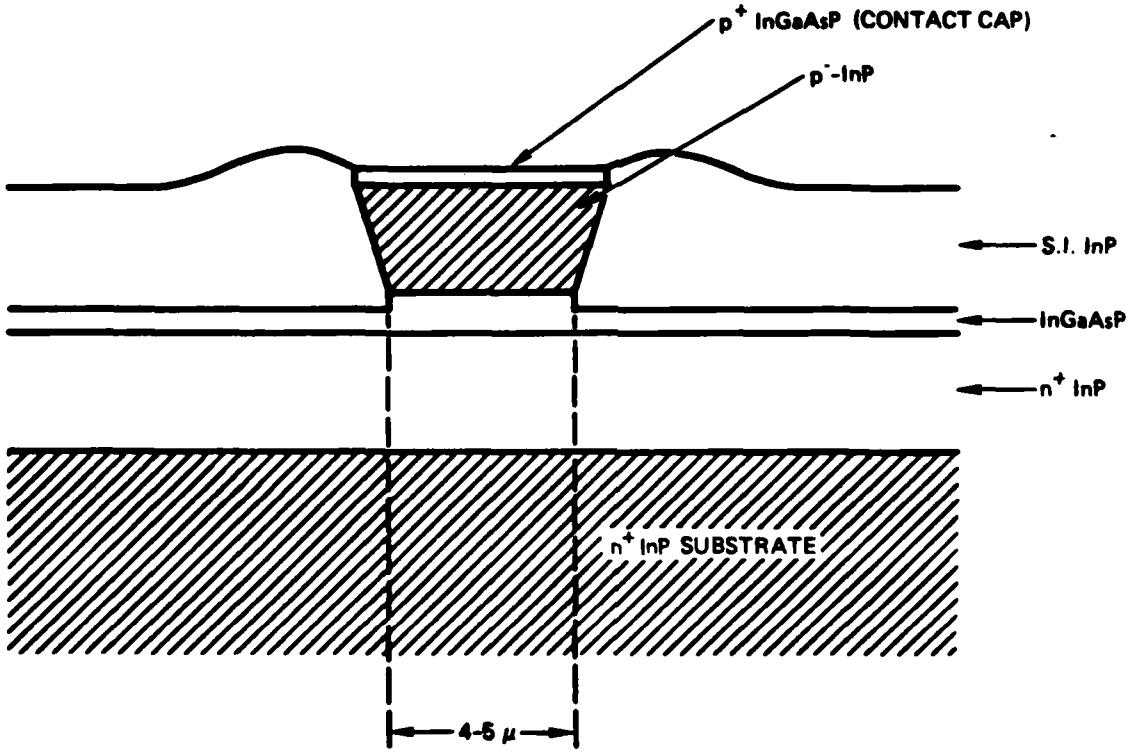

Figure A2. High Power Strip-Loaded Laser.

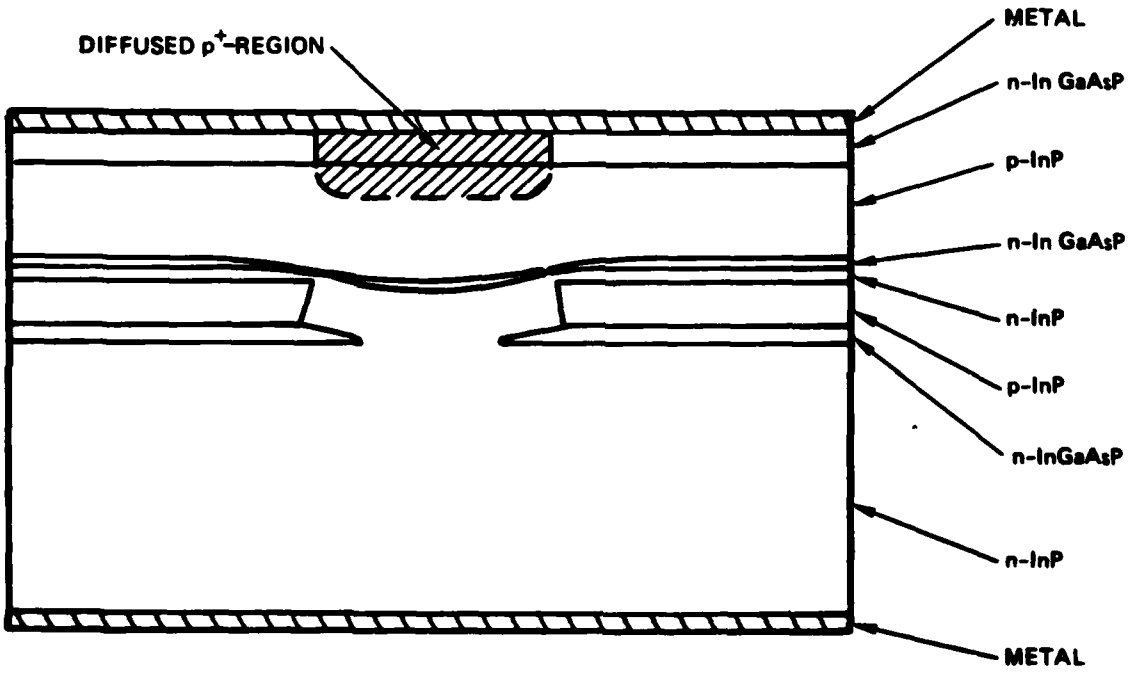

Figure A3. Curved Waveguide Laser.